Basin Research

WILEY

Basin Research IAS EAGE

RESEARCH ARTICLE OPEN ACCESS

Sun, Sea and Sand; Cretaceous Source to Sink Systems of Senegal, NW Africa

M. Pearson[1,2] | M. Casson[1,3] | V. Pashley[4] | J. Redfern[1]

[1]North Africa Research Group (NARG), Department of Earth and Environmental Sciences, The University of Manchester, Manchester, UK | [2]Mineralogy Facility, British Geological Survey, Nottingham, UK | [3]Equinor ASA, Sandsli, Norway | [4]National Isotope Geoscience Laboratory, Kingsley Dunham Centre, Nottingham, UK

Correspondence: M. Pearson (iaian1@bgs.ac.uk)

Received: 22 May 2024 | **Revised:** 18 November 2024 | **Accepted:** 21 November 2024

Funding: The authors received no specific funding for this work.

Keywords: climate | Cretaceous | heavy mineral | Mauritanides | provenance | Senegal

ABSTRACT

Paleo source to sink system analysis requires a complete earth systems model approach, utilising regional geology, tectonics, climate and modern-day source to sink analogues. This study examines the Cretaceous source to sink systems of Senegal, NW Africa, integrating a broad regional dataset using a multidisciplinary mineralogical approach. The most significant regional geological and tectonic events to affect Senegal since the Pan-African Orogenies (800–520 Ma) are the Hercynian Orogeny (320–290 Ma), Pangea break-up and rifting between S. America and Africa, with associated Central Atlantic Magmatic Province volcanism (200 Ma) and uplift of the Mauritanide hinterland (113–66 Ma). In addition to tectonic controls, climate is the principal driver for paleo-drainage reorganisation. During the Cretaceous an antithetical shift in climate from warm and arid (145–115 Ma), to hot and humid (100–88 Ma), increased fluvial catchment and energy. Antecedent paleo-drainage of the Cretaceous Senegalese Basin is governed by subsurface grabens striking hundreds of kilometres into the continent formed during Atlantic rifting. Early Cretaceous aridity restricted fluvial catchments to recycling pre-Cretaceous basinal sediments. Climate change triggered expansion of paleo-drainage catchments during the Aptian caused fluvial incision and erosion of the Gaouâ Group Hercynian to Pan-African age source rocks along the western flank of the Mauritanides. Exhumation increased significantly throughout the Cretaceous Thermal Maximum during the Cenomanian–Turonian, with exhumation of the Gadel Group Pan-African source rocks, evidenced from a shift between a garnetiferous to staurolitic basin mineralogy. Inclusion of 200 Ma zircons into the central Senegalese Basin during the Albian is evidence of possible catchment shifts to include CAMP detritus from the Fouta Djallon Plateau. Cretaceous basinal sediments are almost exclusively sourced from the Mauritanide belt which includes Hercynian metamorphic host rocks and Palaeozoic sediments ultimately derived from the erosion of the Pan-African orogenic belts. During the Maastrichtian, the central fluvial systems breached the southern Mauritanides, sourcing Cambrian zircons from the south.

1 | Introduction

Source to sink system studies encapsulate a host of fundamental geological, tectonic and climatic principals (Morton 2012). In its simplistic form 'source' is typically termed to describe an erosional terrane host to the exhumed sediment of the parental rock or sediment. The source catchment may include single or multiple erosional terranes which can interchange, expand or contract depending on tectonic, climatic or geomorphological forces. The 'sink' is a term used in the characterisation of

Summary

- The Mauritanide Belt is the principal source for Cretaceous basinal sediments.
- Shifts in detrital heavy mineral assemblages exemplifies unroofing of the Mauritanides.
- Antecedent drainage linked to aulacogens and E–W trending grabens striking into the African continent.
- Peak denudation occurred between the Albain and Turonian due to extreme antithetical change in climate from arid to humid.
- Late Cretaceous sediment delivery was restricted to the onshore basin due to the evolution of a swamp-like environment.

sedimentary basins host to the accumulated sediments. These basins can be defined as tectonic, structural, drainage and endorheic (Evenick 2021), each with the potential for burial, compaction and lithification including the propensity for recycling (Morton 2012). Sediment routing systems define how the sediment is transported between the source and sink which can include aeolian (Farrant et al. 2018), fluvial (Mounteney et al. 2021), submarine (Casson 2020) and glacial processes (Latimer et al. 2006). Determination of the sedimentary provenance can link source and sink but not necessarily the sediment pathways undertaken. Deciphering the sediment routing requires a greater understanding of paleo tectonic, climatic and geomorphological forces which can affect catchment size, energy, longevity and intensity of exhumation rates and sediment dispersal.

This research focuses on the provenance of Cretaceous sediments within the Senegalese segment of the Mauritania-Senegal-Guinea-Bissau-Guinea-Conakry (MSGBC; Figure 1) Basin in order to reconstruct sediment routing pathways between the Cretaceous source and sink.

1.1 | Motivation

Hydrocarbon potential of the MSGBC Basin is still poorly constrained despite recent successes with the discovery of the Sangomar Field (formerly SNE) in Senegal and later the Tortue cluster of gas discoveries that straddles the Senegal/Mauritania border. Historically, exploration of Cretaceous sandstone reservoirs along the Northwest African-Atlantic Margin (NWAAM) has had mixed success due to limited basin-wide understanding of the depositional systems (Brownfield and Charpentier 2003; Hathon 2018; Casson 2020; Casson, Calvès, et al. 2020). In 2014, Cairn Energy encountered hydrocarbons in the MSGBC Basin with the FAN-1 well. This prospect targeted late Albian axially reworked contourites and gravity deposits located approximately 100 km offshore in the Sangomar Deep block. In 2017, Cairn Energy drilled the SNE prospect located on the shelf margin and discovered oil. Now called the Sangomar field, it is operated by Woodside, with Phase 1 recoverable reserves estimated at 180 MMBO and up to 250 MMBO in-place resources in addition yet to be exploited (Brownfield and Charpentier 2003). These reservoirs are in Early Albian sands from a pro-delta turbidite apron and delta-fed ramp (Martin et al. 2010; Hathon 2018; Effimoff and Keall 2018). Reliable high-resolution modelling of sediment routing from a multi-sourced system from source to sink requires accurate mineralogical identification of sediments with a high degree of spatial and temporal variation; this ultimately improves the interpretation of depositional systems in order to de-risk understanding of reservoir distribution and quality (Hawie et al. 2015, 2021).

1.2 | Previous Research

Much of the research on the regional structure, geology and basin evolution was published during the late 1980s including papers by: Burke (1976); Page (1988); Ponsard, Roussel, and Villeneuve (1988); Chamley, Debrabant, and Flicoteaux (1988); Fliocoteaux, Latil-Brunt, and Michaud (1988); Ritz and Bellion (1988); Bellion and Crevola (1991); Villeneuve and Cornee (1994). More recent regional publications on the MSGBC Basin include work on the seismic stratigraphy and basin evolution by Mourlot et al. (2018), a review of the petroleum geology of the MSGBC Basin by Ndiaye et al. (2016) and Ko (2018) and a number of re-appraisals of the structural geology: Davison (2005); Villeneuve (2008); Caby and Kienast (2008) and Villeneuve et al. (2015). With renewed interest in the NWAAM, detailed assessments of the regional framework by Gouiza et al. (2019) predicted post-rift uplift and exhumation of the NWAAM hinterland through low-temperature thermochronology analysis of basement rocks from the Mauritanides and surrounding regions. Mourlot et al. (2018) represents the only provenance-based research within the Senegalese region. They utilised provenance indicators based upon Nd/Sr isotopes, and major and trace elemental analyses by ICP-OES which identifies changes in provenance associated with the opening of the Southern and Equatorial Atlantic oceans, and tectonic uplift of the continental hinterland. Assumed Cretaceous paleo-drainage of the Senegal Basin was characterised by indeterminate east–west flowing rivers, with source catchments evolving from the Mauritanides during the Early-Mid Cretaceous to include the Taoudeni Basin, Kédougou-Kéniéba Inlier (KKI) and the upper limit of the Leo-Man Shield during the Late Cretaceous. Drainage reorganisation during the Cenomanian–Turonian was assumed to have resulted from marine transgression of the onshore Senegalese Basin, potentially reaching as far as the Palaeozoic and Hercynian proximal sources (i.e., Mauritanides). Evidence of this global transgression was cited from Schlanger and Jenkyns (1976). However, work by Pearson et al. (2023) cast doubt on the impact of this major Cenomanian–Turonian transgression in Senegal as evidenced by offshore deltaic fan-systems, an absence of significant change in sedimentary facies and potential differences in sedimentary provenance between northern and central/southern fluvial systems.

1.3 | Knowledge Gaps

This research contributes to a larger study to refine our understanding of depositional environments and sediment routing, including; quantitative seismic geomorphology of offshore Gambia (Casson 2020), tectono-stratigraphic evolution of the Mesozoic continental margins of the Central Atlantic,

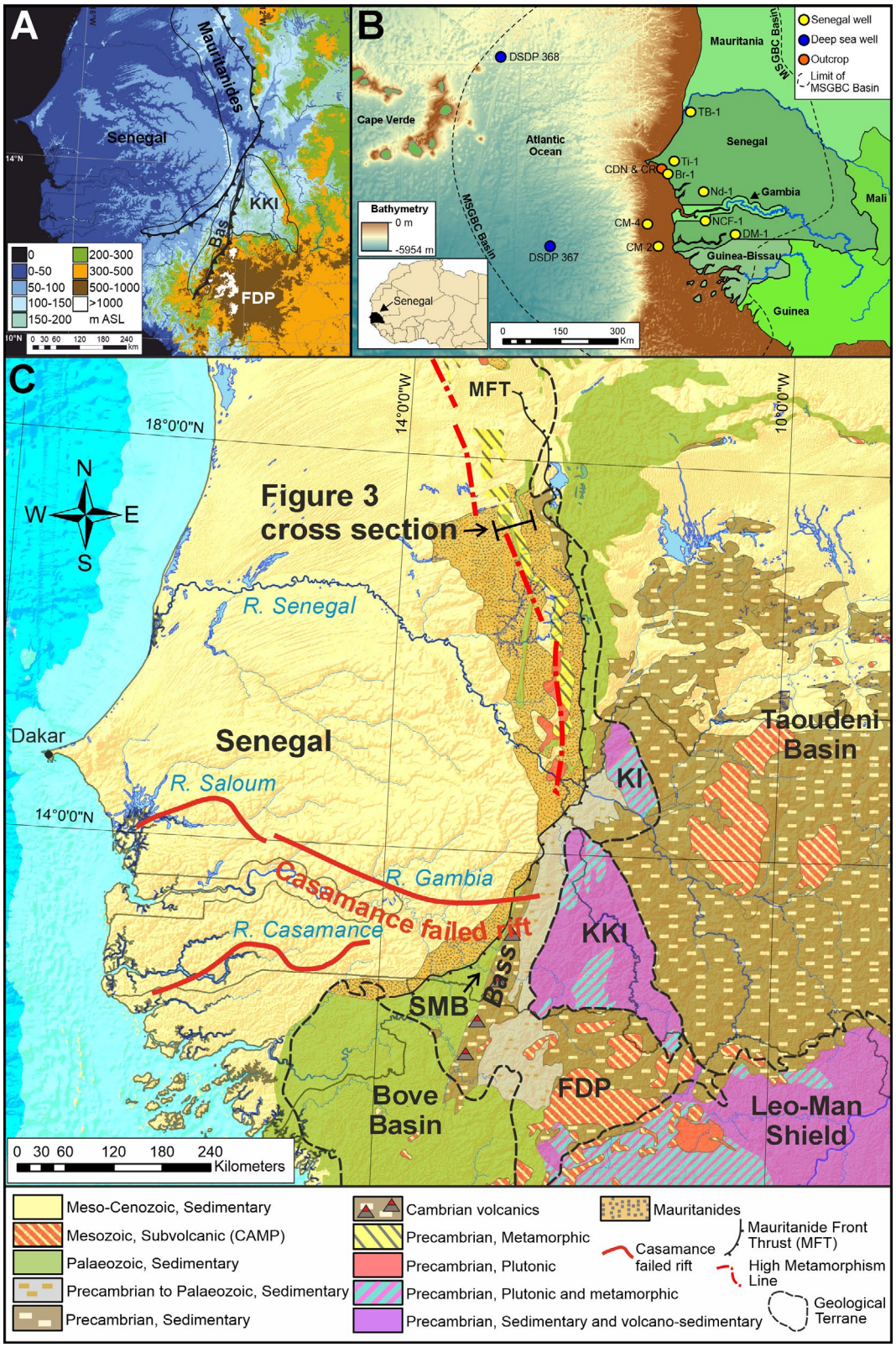

FIGURE 1 | Regional location map of study area (A) digital elevation model (m Above Sea-Level; GEBCO 2021) of Senegal. (B) Location of DSDP wells, nearshore exploration wells and onshore Maastrichtian outcrops. (C) Geological terranes of Senegal modified from Casson (2020) and Mounteney et al. (2021). Bass, Bassaride Belt; FDP, Fouta Djallon plateau; KI, Keyes inlier; KKI, Kédougou-Kéniba inlier; MFT, Mauritanide front thrust; SMB, Salémata meta-basalts.

(Casson 2020) and mixed contourite-turbidite systems offshore Senegal and the implications for palaeoceanography, basin evolution and sediment distribution by Coskun et al. 2023, all providing valuable information for the identification and modelling of Cretaceous sediments offshore Senegal. Most recently, in a linked study to this paper, a modern-day source to sink

study on Cenozoic to modern-day sediments was conducted by Mounteney et al. (2021), as a modern-day source to sink proxy. Understanding Cretaceous climate change of NW Africa is critical for constructing Cretaceous source to sink models, research was undertaken by Pearson et al. (2023) to correlate shifts in climate to changes in clay-mineralogy from basin sediments.

2 | Objectives

This study has assembled an extensive dataset, encompassing a high degree of spatial and temporal variation (Figure 1B) throughout the Cretaceous Senegalese Basin. Analytical methods employed in this research include: detrital heavy mineral analyses, Qm-F-Lt petrography, garnet speciation and U/Pb geochronology of detrital zircons. The integration of several mineralogical methodologies offers the most robust method for establishing sediment provenance (Mange and Morton 2007; Farrant et al. 2018; Roquette et al. 2019; Nauton-Fourteu, Tyrrell, and Morton 2020; Mounteney et al. 2021).

Following a multidisciplinary approach integrating a variety of mineralogical, geochemical and isotopic datasets, alongside extensive literature reviews the aim of this research is to ascertain significant shifts in Cretaceous sedimentary provenance to produce high-resolution source to sink models for the exhumation, transportation and deposition of Cretaceous sediments into the onshore and offshore Senegalese basins. This research will ultimately aid reservoir classification and increase our understanding of Cretaceous source to sink dynamics in this region.

Significant changes in basin mineralogy, geochemistry and geochronology will be linked to changes in climate, environmental conditions, tectonic-frameworks, dynamic topography and paleo-drainage evolution as described in published research.

2.1 | Regional Geology and Tectonism

The Senegalese segment of the MSGBC basin is an 'Atlantic-type' passive margin that developed in the Late Jurassic to Cretaceous following Triassic to Early Jurassic rifting and continental break-up. Comprising of an extensive prograding wedge of Mesozoic–Cenozoic sediments, which develops a broad shelf offshore, formed on a Jurassic carbonate platform that was prograded by Cretaceous clastic sediments (Pearson et al. 2023 and references therein). Onshore, the average maximum thickness of Cretaceous sediments is *ca*. 3 km, with an offshore average maximum thickness of *ca*. 2 km on the shelf thinning over a distance of *ca*. 300 to *ca*. 1 km, drilled by DSDP 367 (Chamley et al. 1983), where present day water depth reaches *ca*. 3 km.

The western margin of the West African Craton (WAC) is a polyphase mobile zone encompassing the Rokelide and Bassaride belts through the Pan-African I (*ca*. 650 Ma) and II (*ca*. 575–580 Ma) orogenic phases (Table 1; Figure 2B; Villeneuve 2008). The hinterland of the MSGBC Basin to the east and southeast is surrounded by the Mauritanides; a *ca*. 1500 km long orogenic belt (Villeneuve et al. 2015) that developed as an accreted orogenic terrain cross-cutting these Pan-African belts during the Late Carboniferous to Early-Permian during the Hercynian Orogeny (320–290 Ma; Figure 2A) with thermal overprinting recorded at 300–325 Ma (Caby and Kienast 2008). The Mauritanides can be divided into two segments; the northern segment, which resides north of the KKI with a width of *ca*. 150 km, whilst the southern segment is approximately 50 km wide (Figure 3C). This regions' tectonic and metamorphic characteristics are locally complicated recording several tectonic events. The Mauritanides are host to Pan-African I basement rocks, including granites, quartzites, garnet–kyanite–staurolite grade mica schists (Dia 1984; Page 1988; Caby and Kienast 2008; Villeneuve 2008; Markwitz, Kim, and Miller 2015). Two main metamorphic domains are acknowledged within the Mauritanides: (1) 'moderately' metamorphosed domain to the east and (2) an 'intensively' metamorphosed terrane to the west (Page 1988; Villeneuve 2008). The limit between these domains is described as the high metamorphism line (Villeneuve 2008; Figures 1C, 3 and 14). The 'intensively' metamorphosed domain was defined by Caby and Kienast (2008) as the Gaouâ Group; a polymetamorphic domain with undetached Palaeozoic quartzite cover with Hercynian age overprint. The 'moderately' metamorphosed eastern domain is sharply bounded to the west by the major west-dipping thrust of the Gadel Group consisting of two units: (1) a gneissic basement and (2) a locally undetached monometamorphic cover referred to as the Farkâkâ Formation consisting of metapelite lithologies of Pan-African age (640 Ma; Caby and Kienast 2008).

East of the southern-Mauritanide Belt is the Bassaride Belt, an NNE–SSW trending orogenic belt formed between the Late Proterozoic and Cambrian (660–520 Ma) linked to the Pan-African II event and the Cadomian orogeny (Villeneuve et al. 2015). The majority of the Bassarides are concealed beneath Palaeozoic sediments, with only small regions of the belt exposed (Figures 1C and 2B). It is characterised as a continental collisional belt, with the earliest recorded metamorphism dated at 660 Ma (Villeneuve 2008). It is composed of amphibolites, micaschists, chlorite-schists, metabasalts, metadolerites, serpentinites, red jaspers and quartzophyllitic rocks.

TABLE 1 | Geological scheme of the West African Craton adapted from Villeneuve et al. (2014).

Periods	Belts
Ordovician to Devonian (320–290 Ma)	Mauritanide Belt (Hercynian)
Late Proterozoic to Cambrian (635–520 Ma)	Rokelide Belt (Pan-African-II)
Cryogenian (850–650 Ma)	Bassaride Belt (Pan-African-I)
Birimian to Archean basement (3–2.5 Ga)	Leo-Man Basement

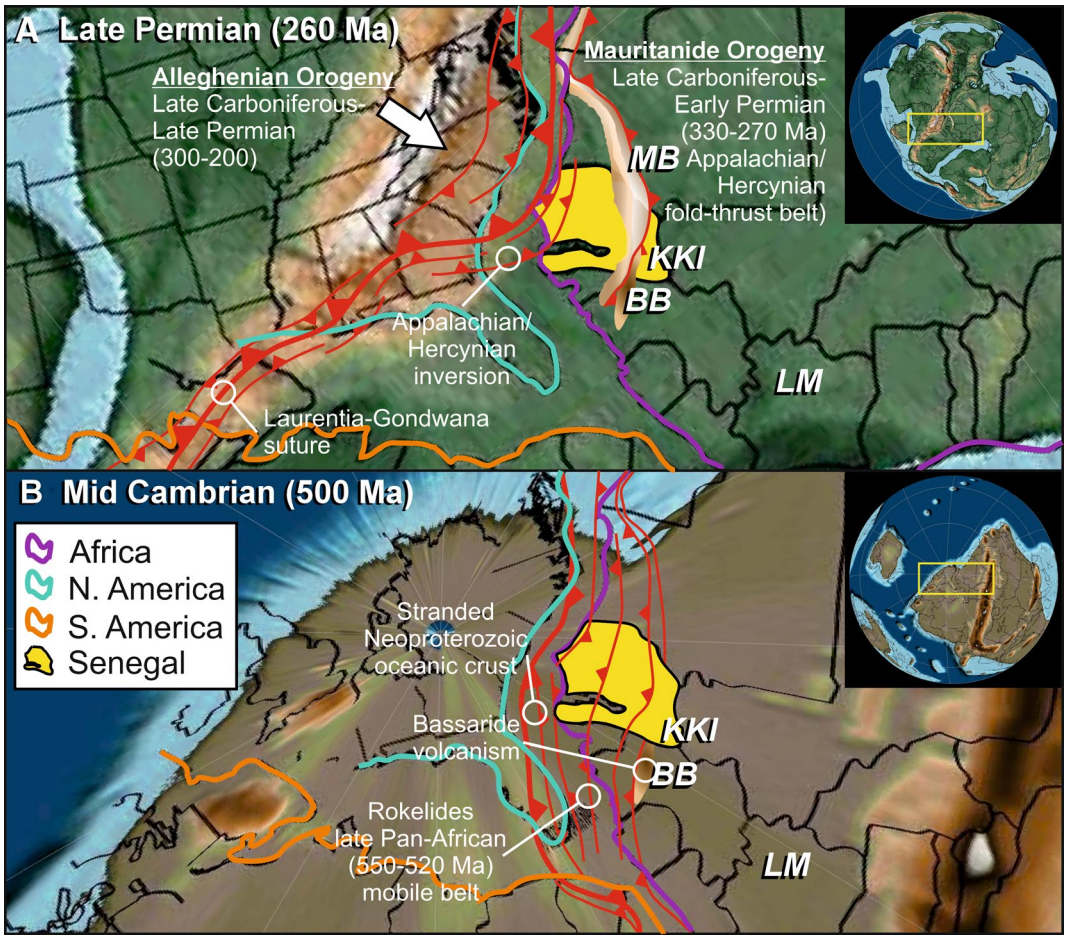

FIGURE 2 | Plate-tectonic reconstructions, based on GPlates palaeogeographical interpretations (Scotese 2016). (A) Late Permian (260 Ma) and (B) Mid. Cambrian (500 Ma). BB, Bassaride Belt; KKI, Kédougou-Kéniba inlier; LM, Leo-Man Shield; MB, Mauritanide Belt.

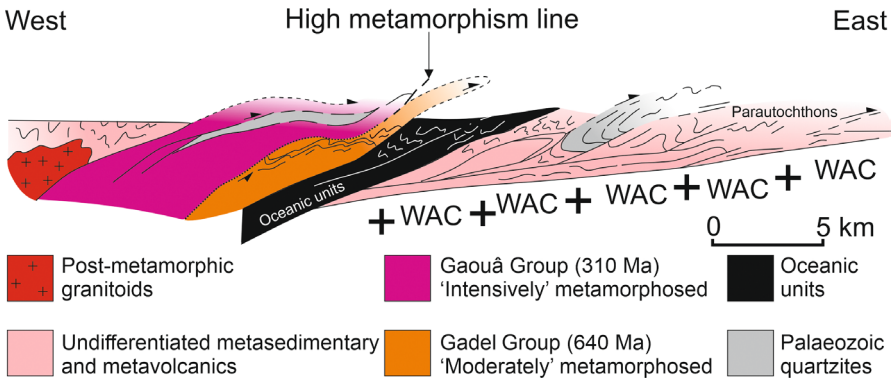

FIGURE 3 | Synthetic geological profile across the Mauritanian segment of the Mauritanide Belt from Caby and Kienast (2008)—line of section displayed on Figure 1C. WAC, West African Craton.

Post collisional volcanism (Figure 2B) occurred throughout the Early Cambrian (Tichilit-al-Beida Group) on the southern margin of the Bassarides, depositing volcano-sedimentary formations over a large area (Nagara and Bouly Groups; Villeneuve 2008). A series of Late Cambrian (494 ± 5.2 Ma) basalt intrusions (Nandoumba Group) are also recognised to have occurred throughout the Bassarides (Villeneuve et al. 2014). Small occurrences of low-grade metamorphosed basalts are located within Salémata region of southern Senegal in contact with the greenschist nappes of the Bassaride Belt (Figure 1C; Fullgraf et al. 2013).

The KKI consists of Paleoproterozoic age volcanic and volcano-sedimentary rocks intruded by granitoids with a wide compositional spectrum (Gueye et al. 2007). During the Late Eburnean Orogeny (~2.16 to ~2.11 Ga) the KKI was deformed by a network of ductile shear-zones (Senegal-Mali shear zone; Ledru et al. 1991; Milési et al. 1992) metamorphosing almost all the

lithostratigraphic units to greenschist facies (Gueye et al. 2007). Resulting skarn-type mineralisation occurred throughout the Late Eburnean orogeny, hosting various deposits of including iron-ore and gold (Markwitz, Kim, and Miller 2015; Gerson et al. 2018), containing accessory metasomatic (Type D) garnets (Mounteney et al. 2021).

2.2 | Modern-Day Rivers and Catchment

The modern-day Senegal river is the largest of the four major tributaries flowing through Senegal, followed by the Gambia, Casamance and Saloum rivers (Figure 1). The Senegal is the only river actively eroding and transporting fresh detritus from the western-WAC. The modern-day Senegal River cuts through the Mauritanides just north of the KKI, where several tributaries of the river have their source catchment in the WAC (Figure 1). The catchment includes eroded sediment from the northern extent of the Fouta Djallon Plateau (FDP), KKI basement rocks, including granites, quartzites and staurolite/garnet-grade mica schists, eclogite and greenschist facies from the Mauritanides and Phanerozoic sediments of the Taoudeni Basin (Mounteney et al. 2021 and references therein; Figure 1C). The remaining three river systems are actively recycling Meso-Cenozoic sediments from within the onshore Senegal Basin (Mounteney et al. 2021).

2.3 | Cretaceous Climate

At the onset of the Early Cretaceous the climate has been interpreted to be arid (Scherer et al. 2020; Dou et al. 2023), with only limited monsoonal geostrophic precipitation restricted to upland coastal regions. Continued fragmentation of Gondwana led to the disruption of a large low-pressure cell in the southern hemisphere, leading to the development of an equatorial tropic zone influenced by Hadley cell circulation (Scherer et al. 2020). The NW African equatorial climate subsequently evolved into hothouse conditions which persisted throughout the Cenomanian and into the Early Coniacian, referred to as the Cretaceous Thermal Maximum (CTM; Haq and Huber 2017). This period of climate change has been interpreted to be caused by several factors, including: the continued fragmentation of Gondwana, the opening of the Equatorial Atlantic Gateway (Pletsch et al. 2001), expansion of the equatorial tropics (Hay and Floegal 2012), accelerated magmatism from the Central Atlantic Magmatic Province (CAMP; Takashima et al. 2006) and the eruption of several Large Igneous Provinces (LIPs; Buchs et al. 2018). Whilst exceptional humidity defined the CTM (Held and Soden 2000; Pierrehumbert 2002), its demise and the subsequent return to a 'normal' Cretaceous climate, was also in-part caused by the high humidity, due to an extreme hydrological cycle causing prolonged and exceptional carbon sequestration through photosynthesis and increased silicate weathering (Heimhofer et al. 2018). However, this was not the only mechanism which acted as a driver to allow the Earth's climate to exit its hothouse state. Many authors suggest the CTM was at least in-part caused by tectonics (Perez-Díaz and Eagles 2017) and the ultimate departure from this hothouse period was due to the continued drifting apart of Africa and S. America, which resulted in the expansion of the Equatorial Atlantic Gateway, increasing the size of the water body (Hay et al. 2019), and allowing deep water currents to form. This is interpreted to have initiated a halokinetic ocean current between the hypersaline Northern Atlantic Basin and fresher waters from the southern hemisphere, (Hay 2009; Poulsen, Gendaszek, and Jacob 2013; Perez-Díaz and Eagles 2017) allowing the transfer of equatorial heat towards the comparatively cooler polar regions. Towards the end of the Cretaceous palynological analysis of Maastrichtian Senegalese spores (Salard-Cheboldaeff and Dejax 1991) indicated a transition to hot and damp ecological conditions with extensive vegetation established around lakes and swamps.

3 | Material and Methods

3.1 | Material

Samples of sandstone from core and cuttings were analysed from a suite of eight onshore and offshore exploration wells from Senegal (Figure 1B, Table 2). Senegalese exploratory well samples were collected from the PETROSEN core repository, Dakar, Senegal. A single sample of fine-grained sand of Albian age

TABLE 2 | Location of samples collected from exploration wells (exp-well) and outcrop.

Region	Location name	Location ID	Latitude	Longitude
Onshore Senegal Basin exp-well	M'Bour-1	Br-1	14°25′0.75′N	16°58′1.11 W
Offshore Senegal Basin exp-well	Casamance Maritime-4	CM-4	12°45′27.10″N	17°24′43.14″W
Onshore Senegal Basin exp-well	Diana Malari-1	DM-1	12°49′42.42″N	15°11′16.31″W
Onshore Senegal Basin exp-well	Nord Casamance F-1	NCF-1	13°10′18.57 N	15°59′58.53 W
Onshore Senegal Basin exp-well	N'Dofane-1	Nd	13°56′23.14″N	16° 2′59.99″W
Onshore Senegal Basin exp-well	Toundou-Besset-1	TB-1	16°13′3.38″N	16°23′12.94″W
Onshore Senegal Basin exp-well	Tienaba-1	Ti-1	14°47′17.88″N	16°42′35.76″W
Senegal coast outcrop	Cap Rouge	CR	14°38′6.46″N	17°10′24.33″W
Senegal coast outcrop	Cap de Naze	CdN	14°32′19.36″N	17°6′15.28″W
Cap Verde Basin, offshore Senegal exp-well	Deep Sea Drilling Programme 367	DSDP 367	12°29.2′N	20°02.8′W

was collected from well DSDP 367. Samples were also collected from Maastrichtian shallow marine sandstones from coastal exposures at Cap de Naze and Cap Rouge (Pearson et al. 2023; Figure 1B). Sediment ages are determined from biostratigraphic dating defined by PETROSEN well-reports.

3.2 | Heavy Mineral Analysis

Traditionally, heavy mineral analysis has been performed on the fine-sand fraction of sediments through the methodology defined by Morton (1985) and Knox, Soliman, and Essa (2011). This methodology is still employed in recent provenance-based studies (Caracciolo et al. 2014; Farrant et al. 2018; Nauton-Fourteu, Tyrrell, and Morton 2020; Mounteney et al. 2021) and has been chosen in order to correlate provenance signatures between this research and the data from Mounteney et al. (2021). The 63–125 μm grain size encapsulates the highest variety of detrital heavy mineral species, demonstrating the usefulness of analysing this grain-size window (Krippner et al. 2015). Detrital heavy mineral assemblages are principally governed by the origin of the source rock lithology; however, this can be extensively modified through hydrodynamic processes during transportation, weathering and diagenesis. Hydrodynamic affects associated with fluvial transportation are minimised through the selective identification of heavy minerals within the 63–125 μm range (Morton 2012).

Heavy mineral separation was performed using lithiumheteropolytungstate at a measured density of 2.9 g/cm^3, separating grains using a sink-float method (Mounteney 2011). Identification of transparent detrital heavy minerals was performed using a transmitted light microscope, averaging counts of 400 transparent detrital heavy minerals where possible.

Heavy mineral indices are used to complement the component mineral assemblage (Figures 4–6) in order to better constrain sediment provenance (Morton and McGill 2018). Whilst the component mineral assemblage can be diagnostic of the inherited source terrane; subaerial, transportational and depositional modification of the detritus can alter the resultant heavy mineral signature. The utilisation of heavy mineral indices, as described by Morton and Hallsworth (1994), provides a balanced perspective of sedimentary provenance. It focuses on the relative abundance of detrital heavy minerals that are stable during diagenesis, which possess similar hydraulic properties. For the purpose of this study defined heavy mineral indices include: staurolite:tourmaline index (STi), garnet:zircon index (GZi) and rutile:zircon index (RZi).

Samples analysed from exploratory wells Br-1, CM-4, NCF-1, Nd-1, TB-1 and DSDP 367 are used to constrain Cretaceous sedimentary provenance. Samples taken from the Maastrichtian Cap Rouge and Cap de Naze outcrops are composed of shallow marine sands deposited across the Senegalese shelf as stacked progradational para-sequences of shallow marine sandstones and shelfal siltstones (Barusseau et al. 2009, Casson, Calvès, et al. 2020). The well DM-1 encountered the oldest sediments in the study (Silurian to Devonian) and was chosen to provide a comparison between Palaeozoic and Mesozoic provenance which may provide data on Palaeozoic sedimentary provenance.

3.3 | SEM Mineral Speciation

Heavy mineral speciation of garnet was performed using a FEI Quanta 600 scanning electron microscope fitted with an Oxford Instruments XMax 50 mm^2 silicon-drift energy dispersive x-ray (EDX) detector. Analytical conditions for the scanning electron microscope were high vacuum (< 10–4 Torr), an accelerating voltage of 20 keV, and a spot size of 6 (beam current ~2 nA). Automated quantitative microanalysis and mineral identification was performed using the 'Feature' package within the INCA software. Multiple images were obtained over a mm-scale grid with the backscatter electron (BSE) technique. Since the brightness of a phase under BSE imaging is proportional to its mean atomic number, greyscale thresholding was used to limit microanalysis to grains with similar average greyscale values to that of known garnets. Microanalytical EDX data was obtained from a centre-point site of each of the threshold-identified grains, determined as the centre of the longest chord (a straight line that can be drawn entirely within the grain boundary; Mounteney et al. 2021). The automated nature of this technique allows for a very-high threshold of grain analyses, scanning thousands of heavy minerals in search of garnet, with the highest number of recorded garnets (892) identified in the Aptian sands of Nd-1 (Figure 7F). Whilst grain size has been demonstrated to be a crucial factor in mineral speciation (Krippner et al. 2015), the 63–125 μm fraction was used in order to compare against garnet speciation of modern-day sediments of Senegal (Mounteney et al. 2021).

3.4 | U/Pb Zircon Geochronology

Zircons are analysed at the Geochronology and Tracers Facility, British Geological Survey (GTF-BGS) using a Nu Instruments, Nu Plasma HR, multi-collector inductively coupled plasma mass spectrometer (MC-ICP-MS). The Nu Plasma HR is operated in static mode, with simultaneous measurement of the isotopes of interest on either a Faraday detector or an ETP secondary electron multiplier. Laser sampling is performed using an Elemental Scientific Lasers UC-193 excimer laser ablation system. The ablation parameters are as follows: 20 μm static spot, run at a repetition rate of 10 Hz, with a fluence of ~2.2 J/cm^2. Samples are ablated for 20 s with a 15 s washout/laser warm-up period between each sample. Data are acquired using the time-resolved analysis (TRA) function of the Nu HR's software and processed using Iolite 4; a software package specifically designed to handle the large volumes of data produced by laser ablation multi-collector inductively coupled plasma mass spectrometer (Paton et al. 2011). Isotopic data were exported and plotted using IsoplotR software (Vermeesch 2018) specific parameters are defined in Mounteney et al. (2021).

3.5 | Q-F-Lt Petrography

Petrographic clast analysis of sands and sandstones was performed using the Gazzi-Dickinson method (Decker et al. 1985) and conducted on 300 sand-sized counts per sample. Counts included the identification of monocrystalline and

polycrystalline-quartz, plagioclase and K-feldspar, lithic grains (metamorphic, igneous and sedimentary), clay minerals (muscovite, biotite and chlorite), carbonate, accessory minerals and fine-grained clay matrix (Decker et al. 1985; Li, Qu, and Gong 2015; Dickinson et al. 1983).

3.6 | Grain Petrography

Grain textures are typically manifested as surface pitting, etching and faceting resulting from chemical weathering and/or diagenesis. The most extensive weathering occurs in warm to hot humid climates where chemical reactions proceed at a faster rate through the interaction of acidic meteoric water (Ando et al. 2012) and/or organic acids from tropical soil profiles (Afanasiev et al. 2013). Observation and interpretation of dissolution features in detrital minerals can aid in the understanding of climate, mode of transportation and to the extent that the heavy mineral assemblage may have been modified by diagenesis. Detrital grain morphologies are captured using a petrological microscope under plain-polarised light conditions. Corrosion textures are described using the catalogue of optical grain images defined by Ando et al. (2012). Apatite is the least stable of all the detrital heavy minerals to the effects of subaerial acidic weathering with garnet being mildly susceptible to these conditions. Conversely, apatite is among some of the most resistant detrital heavy minerals to diagenetic dissolution through intrastratal dissolution, whilst garnet is comparatively more susceptible to diagenesis (Morton 2012).

4 | Results

4.1 | Heavy Mineral Analysis

Results from detrital heavy mineral analysis are illustrated in Figure 4. Heavy mineral indices for the four key wells (TB-1, Ti-1, Br-1 and Nd-1) are displayed in Figures 5 and 6.

4.1.1 | TB-1

Early-Aptian heavy minerals are dominated by apatite, tourmaline and zircon with a minor proportion of garnet and rutile. Towards the late Aptian, garnet content increases substantially (39%), peaking during the late Albian (77%). Garnet content declines throughout the Cenomanian, with the concurrent increase of rutile and staurolite towards the end of the epoch. This

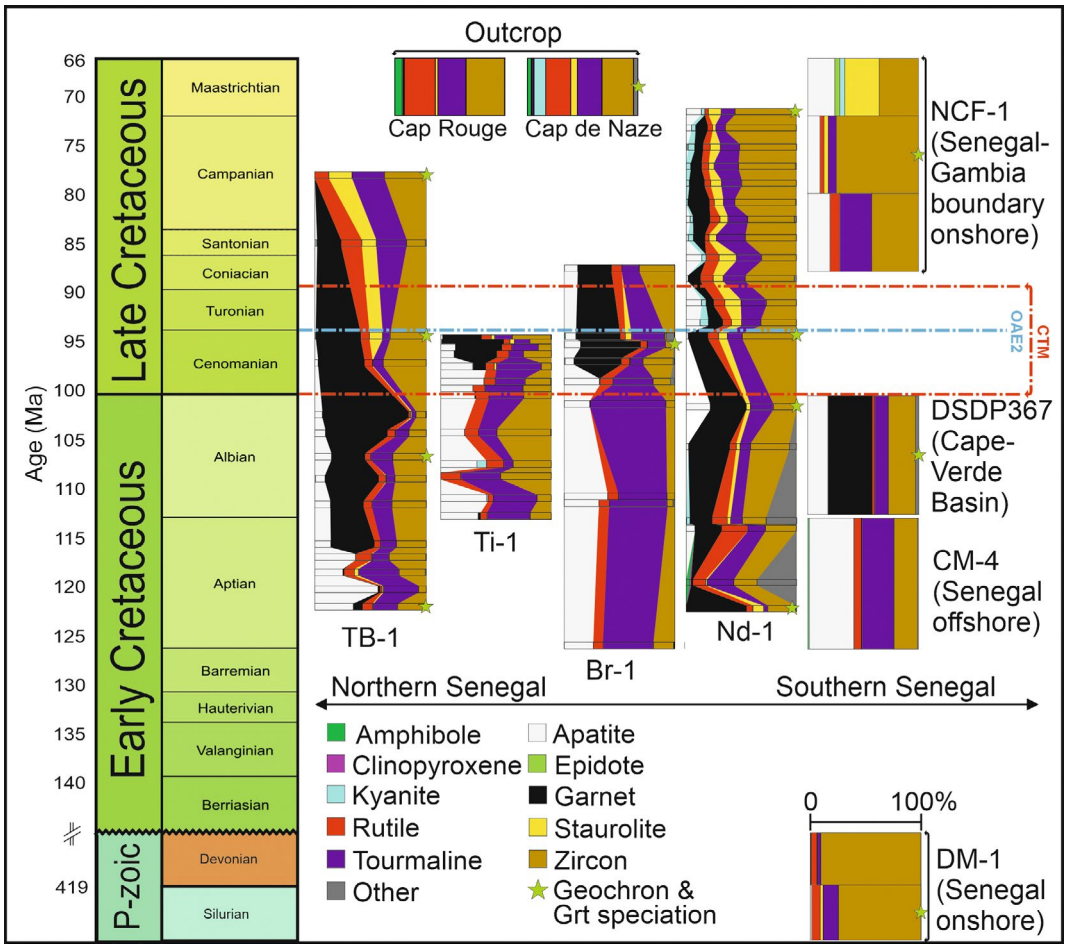

FIGURE 4 | Transparent detrital heavy mineral assemblage, opaque minerals have been excluded. 'Other' includes trace quantities of the following heavy minerals: Anatase, andalusite, baryte, brookite, Cr-spinel, glaucophane, monazite, orthopyroxene, sillimanite, spinel, topaz and titanite. CTM, Cretaceous thermal maximum; OAE, Ocean Anoxia Event-2.

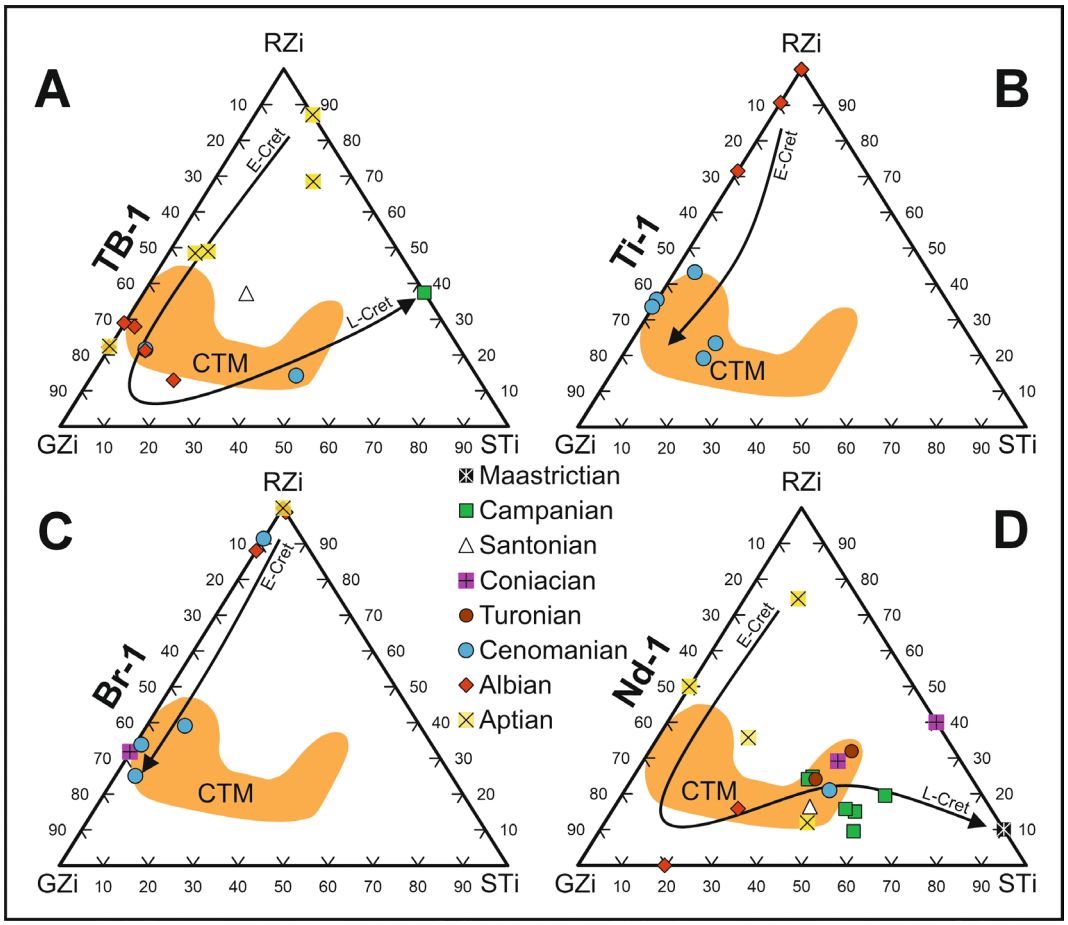

FIGURE 5 | Heavy mineral index ternary plots from wells TB-1 (A), Ti-1 (B), Br-1 (C) and Nd-1 (D). CTM, Cretaceous thermal maximum; GZi, garnet:zircon index; RZi, rutile:zircon index; STi, staurolite:tourmaline index.

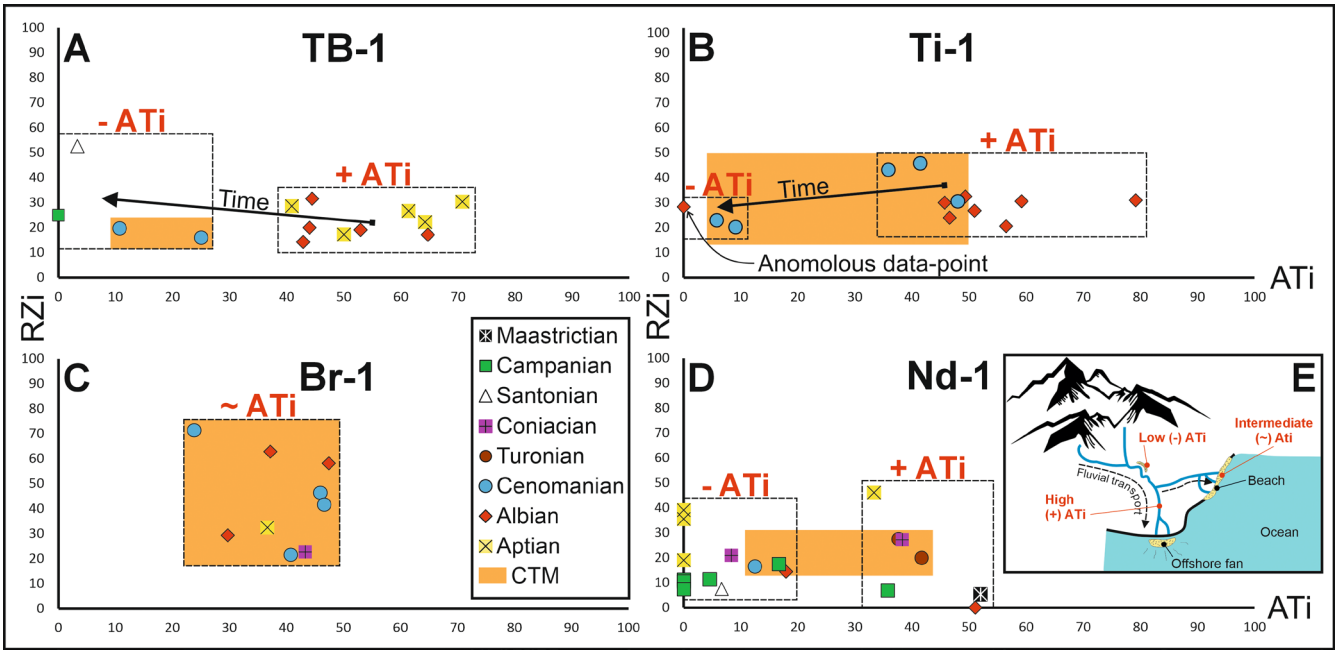

FIGURE 6 | (A–D) Binary plots for rutile:zircon index (RZi) and apatite:tourmaline index (ATi). (E) Schematic representation of a source to sink model differentiating interdistributary bay and mouth bar deposits with low (–) ATi, indicating a long residence time and channelised deposits with a high (+) ATi indicating a short residence time. CTM, Cretaceous thermal maximum.

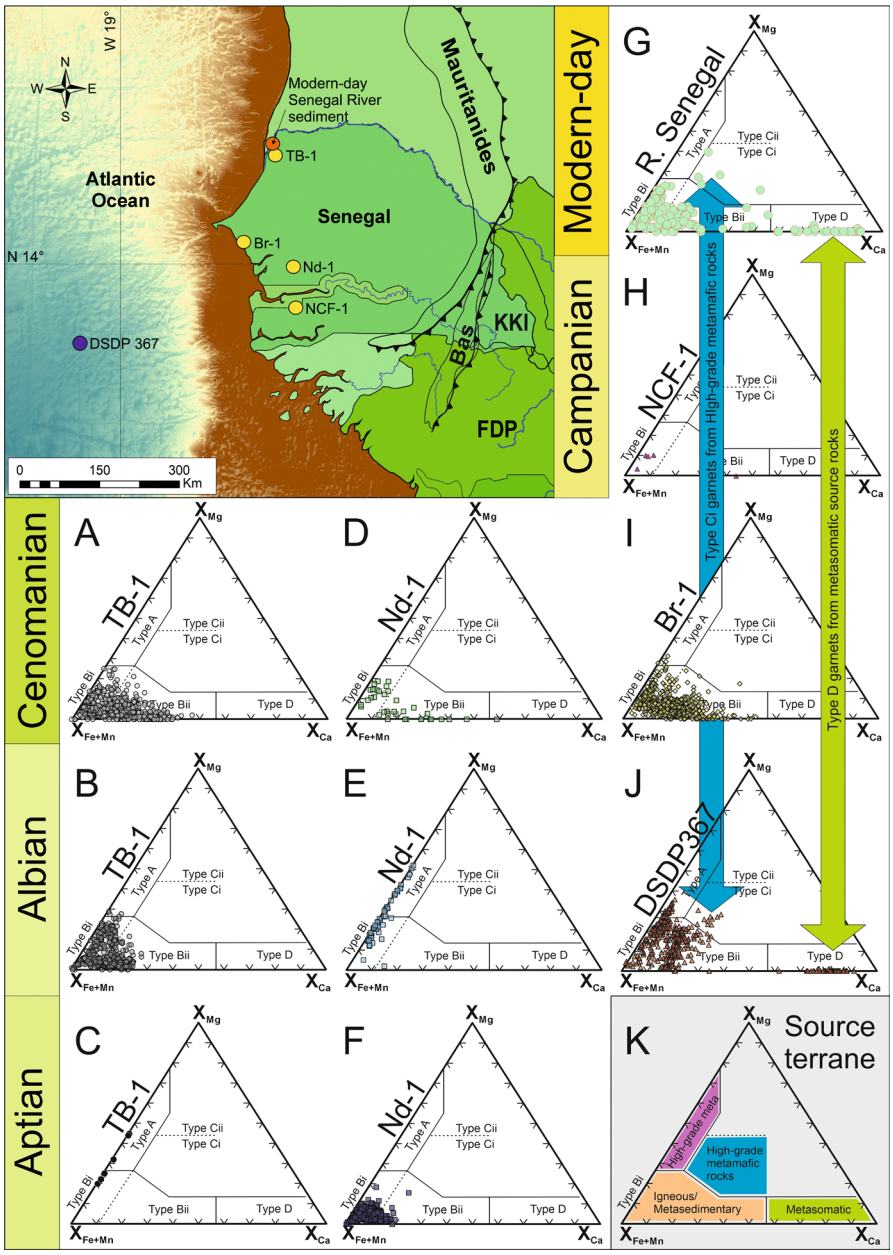

FIGURE 7 | Garnet speciation ternary diagrams, data from geochemical analysis of polished heavy mineral grain mounts, based on the classification scheme by Mange and Morton (2007). Type-A, high-grade granulite-facies metasediments or charnockites and intermediate felsic igneous rocks; Type-B, amphibolite-facies metasedimentary rocks; Bi, intermediate to felsic igneous rocks; Ci, high-grade mafic rocks; Cii, ultramafics with high Mg (pyroxenites and peridotites); D, metasomatic rocks, very low-grade metamafic rocks and ultrahigh temperature metamorphosed calc-silicate granulites. Plots A–F and H–J present garnet speciation from this study, plot (G) presents Senegal River garnet data extracted from Mounteney et al. (2021) and plot K represents garnet type and corresponding source terrane.

trend continues into the Campanian, by which time garnet is absent, with a measured increase in rutile (12%–19%), staurolite (13%–21%) and tourmaline (27%–29%).

4.1.2 | Ti-1 and Br-1

Heavy mineral assemblage for Ti-1 and Br-1 are remarkably similar, however this might have been expected given the proximity of both wells to each other (Figure 1B). Aptian to Lower-Cenomanian assemblages consist of apatite and tourmaline with rutile and zircon. There is a transition to a garnet-rich (11%–55%) assemblage during the middle Cenomanian, with the addition of staurolite during the Cenomanian–Turonian transition.

4.1.3 | Nd-1

The heavy minerals identified in well Nd-1 remain mineralogically comparable throughout the entire succession including variable proportions of apatite (0%–22%), garnet (0%–55%), kyanite (0%–8%), rutile (0%–24%), staurolite (0%–16%), tourmaline (4%–26%) and zircon (21%–64%). The category 'Others' within Aptian and Albian sediments consist of anatase and baryte. The

most significant shift in detrital heavy minerals occurs during the Cenomanian–Turonian transition, whereby garnet content decreases from an average of 27%–9.7%, staurolite increases from an average of 4.8%–9.0% and kyanite increases from 1.3% to 3.7%.

4.1.4 | DM-1

The heavy mineral assemblage is predominantly composed of zircon (Ave. 83%) with a minor proportion of rutile (Ave. 6.4%), staurolite (Ave. 1.6%) and tourmaline (Ave. 8.4%). Within the high concentration of zircons, 10% of total Devonian zircons and 2% of Silurian zircons were pink in colour.

4.1.5 | CM-4

A single Aptian age sediment was analysed from well CM-4, which allowed comparison of onshore and offshore provenance. The heavy mineral assemblage is comparable to well Br-1, predominantly composed of apatite (41%), rutile (6.6%), tourmaline (29%) and zircon (21%).

4.1.6 | DSDP 367

Only a single sample of Albian age sediment was identified to have a measurable proportion of fine sand yielding sufficient heavy minerals for analysis. Heavy mineral assemblage is comparable to Albian sands analysed from well TB-1, consisting of a high proportion of apatite (18%), garnet (39%), rutile (2.2%), tourmaline (12%) and zircon (24.6%).

4.1.7 | NCF-1

Well NCF-1 comprises of two samples of undifferentiated Senonian age (Coniacian to Campanian) and a single Maastrichtian age sediment. Senonian heavy mineral content is predominantly composed of zircon (42%–74%), with tourmaline (7%–29%), apatite (11%–20%), rutile (3%–9%) and staurolite (3.7%) in the Upper-Senonian sediment. The single Maastrichtian sample has an anomalous heavy mineral assemblage, predominantly composed of zircon (36%), staurolite (31%) and apatite (24%) with minor kyanite (4.4%) and epidote (4.4%).

4.1.8 | Cap Rouge and Cap De Naze

The combined heavy mineral assemblages are similar in both outcrops, consisting of zircon (28%–35%), tourmaline (22%–26%), rutile (22%–28%), calc-amphibole (3%–7%), trace quantities of clinopyroxene (0.3%–1.1%) and epidote (0.6%–0.7%). Kyanite (0.3%) and staurolite (2.4%) are trace components in Cap Rouge but is more abundant within Cap de Naze (Kyanite-10.5% and staurolite-5.9%).

4.2 | Heavy Mineral Indices

Heavy mineral indices for wells Ti-1 and Br1 both exhibit high RZi values for Early Cretaceous sediments, transitioning into higher GZi values in the Cenomanian-Coniacian (Figure 5B,C). Indices for TB-1 and Nd-1 (Figure 5A,D) exhibit similar trends in provenance, with high RZi values during the Aptian, shifting towards high GZi values throughout the Albian. A third major shift in provenance occurs during the period of the CTM whereby provenance indices trend towards high STi values.

The apatite:tourmaline index (ATi) can provide valuable evidence on the pre-depositional history of a sediment due to their contrasting stability. Of all the heavy minerals apatite is the most susceptible to chemical weathering under acidic conditions, especially within tropical environments which can be a useful indicator of weathering rates during alluvial storage (Morton 2012); whilst tourmaline is one of the three most stable of the heavy minerals (rutile and zircon being the other two). Due to the similar physical properties of rutile and zircon, including density and resistivity to weathering and diagenesis, the rutile:zircon index (RZi) is considered to be more diagnostic of changes in sediment provenance (Morton and Hallsworth 1999).

RZi values (Figure 6) could infer a similar sedimentary provenance, with the majority of RZi values ranging between 10 and 40, however, this doesn't accurately reflect the true shift in provenance, which is more evident when comparing RZi, GZi and STi values (Figure 5). ATi values for well Br-1 exhibit no discernible relationship with deposition age, with intermediate ATi values. Both wells Ti-1 and Nd-1 display a significant variation in ATi values with a lower value in the range of 0–20 and a higher ATi value in the range of 30–80 (Figure 6B,D), however, these two populations of ATi values exhibit no correlation with depositional age. Well TB-1 ATi values (Figure 6A) are similar to the range of indices exhibited in wells Ti-1 and Nd-1 with an upper ATi population of 40–70 and a lower population in the range of 0–30. High ATi values for TB-1 sediments are exclusively Aptian to Albian in age, whilst the lower ATi values are all younger in age (Cenomanian to Santonian).

4.3 | Garnet Speciation

Garnet speciation is based on the classification scheme devised by Mange and Morton (2007), using Fe, Mg, Mn and Ca compositional discrimination (Figure 7). The relative proportion of Ca-rich grossular garnet is typically concentrated in the smaller grain sizes, whereas Mg-rich pyrope is typically found within the coarser grain-size fractions (Krippner et al. 2015), however given the total number of garnets examined in this study (3337), the total absence of Mg-rich pyrope garnets is more likely to be provenance specific and not dependant on grain size. Indeed, there are many examples for the occurrence of Mg-rich garnets within the 63–125 μm grain size (Lewin et al. 2020; Morton, Chisholm, and Frei 2024). Statistically, if pyrope garnets are present in the coarser fractions there should be a small proportion of broken 'smaller' grossular grains identified within the 63–125 μm but this is not the case. The occurrence of Ca-rich grossular garnets (Type D) in Albian DSDP 367 sediments (Figure 7J) must also be provenance specific and not an artefact of analysing a narrow grain size as they are not identified in any of the other

Cretaceous basinal sands. Aptian garnets recorded from well TB-1 are calcic-poor Type A and Bi, representing an igneous/metasedimentary to high-grade metamorphic origin. The limited garnet data points reflect the low garnet content as seen in Figure 4. Garnet species change to principally Type Bi (igneous/metasedimentary) during the Albian and into the Cenomanian, where the Type Bi garnets transition to include more calcic endmember Type Bi garnets. In well Nd-1, Aptian garnets include Type Bi endmember species but shift to Type A and Bi (igneous/metasedimentary to high-grade metamorphic) during the Albian. Cenomanian garnets recovered from wells Nd-1 and Br-1 are comparable to Cenomanian garnets from well TB-1, both containing Fe + Mn to calcic endmember Type Bi garnets.

Limited data points are available for Campanian garnets recovered from well NCF-1, owing to the garnet-poor heavy mineral assemblage highlighted in Figure 4. Although limited recovery, the garnets still reflect the same source origin, comprising of Type Bi garnets. In the offshore well DSDP 367, recovered garnets of Albian age comprise of several endmember species including: Type A (high-grade metamorphic), Type B (igneous/metasedimentary), Type D (Metasomatic) and Type Ci (high-grade mafic). Whilst the Type A and Bi garnets are identified in other Cretaceous sediments, there are no other occurrences of Type D or Type Ci garnets in any of the other Cretaceous basinal sediments.

4.4 | Grain Textures

Photomicrographs of detrital garnet and apatite grains are displayed in Figures 8–11.

TB-1 Santonian garnet grains (Figure 8A) range in morphology between rounded dodecahedral to blocky grains with minimal surface etching associated with the blockier grains. TB-1 Albian to Cenomanian garnet grains (Figure 8B,C) consist of two types of surface textures including slight-advanced dissolution evidenced by 'microscaly' etch facets and a greater degree of dissolution represented by large-scale cuboid etch faceting. TB-1 Aptian garnet textures (Figure 8D) range between unaltered subhedral dodecahedral to angular-blocky with low degrees of surface etching and large-scale cuboid etch faceted grains. Nd-1 Cenomanian garnet grains (Figure 9A) range in morphology between angular grains with prominent conchoidal fracturing and subrounded to rounded grains both with slight surface corrosion. Nd-1 Aptian to Albian garnet

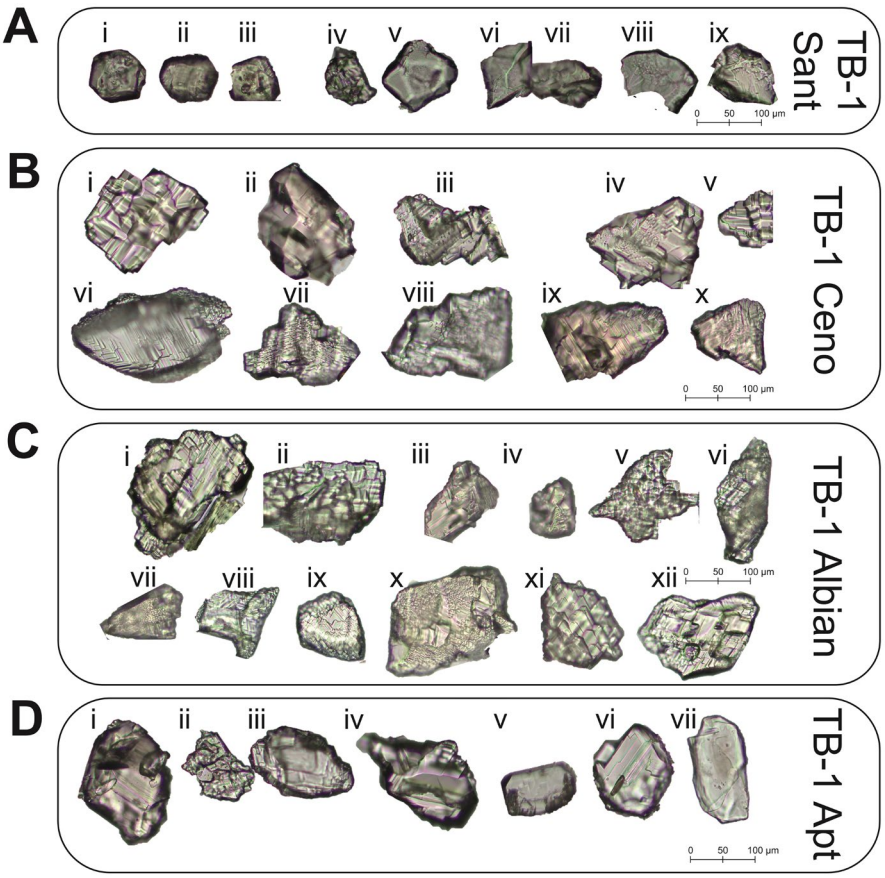

FIGURE 8 | Representative photomicrograph images of garnet observed under plain-polarised light. (A) Santonian, well TB-1 (i–iii) rounded dodecahedral grains, (iv–vii) blocky/fractured grains, (viii) grains showing early-stage corrosion, (ix) surface etch facets on grain surface. (B) Cenomanian, well TB-1 (i–v) large-scale cuboid etch faceted grains, (vi–x) 'microscaly' etch facets on grain surface. (C) Albian, well TB-1 (i–vii) large-scale cuboid etch faceted grains, (viii) early-stage corrosion, (viii–x) 'microscaly' etch facets on grain surface, (xi–xii) macroscaly etch facets. (D) Aptian, well TB-1 (i–iv) large-scale cuboid etch faceted grains (v–vii) blocky grains with low-degree of surface faceting, (viii) subhedral dodecahedral grain.

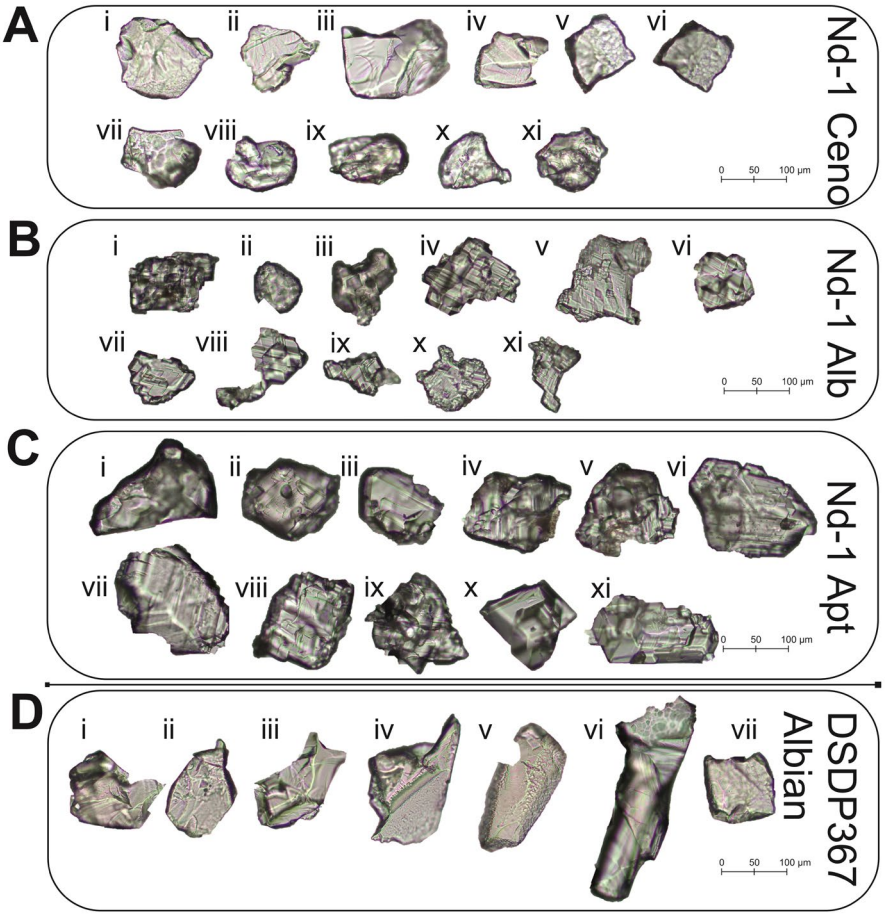

FIGURE 9 | Representative photomicrograph images of garnet observed under plain-polarised light. (A) Cenomanian, well Nd-1 (i–vii) conchoidal fractured grains with slight surface corrosion, (viii–xi) subrounded to rounded grains with slight surface corrosion. (B) Albian, well Nd-1, (i–vi) large-scale cuboid etch faceted grains, (vii–xi) advanced to heavily corroded to skeletal grains. (C) Aptian, well Nd-1, (i–xi) large-scale cuboid etch faceted grains. (D) Albian, DSDP 367 (i–iii) angular grains with conchoidal fracturing, (iv–v) early-stage corrosion, (vi–vii) mamillated surface etching.

grains (Figure 9B,C) exhibit large-scale cuboid etch facets, Albian grains are heavily corroded compared to garnets of Aptian age with several grains showing skeletal morphologies. DSDP 367 Albian garnet grains (Figure 9D) are angular exhibiting conchoidal fracturing with dissolution features ranging from early-stage corrosion to mamillated surface etching to 'microscaly' etch facets.

TB-1 Cenomanian apatite grains (Figure 10A) are subangular with low-sphericity, surface corrosion is absent or initial to slight. TB-1 Albian apatite grain morphologies (Figure 10B) range from subrounded with low sphericity to subangular with high sphericity with the latter grains displaying slight to advanced stages of surface corrosion. DSDP 367 Albian apatite grains (Figure 10C) are subangular to angular with low sphericity and surface corrosion either absent or in the initial to slight stages. TB-1 Aptian apatite grains (Figure 10D) have some angularity but are predominantly rounded with medium sphericity, surface corrosion features are absent. Apatite's from well Br-1 (Figure 11) exhibit a range of morphologies and textures unconstrained to age and depth of sediment. Morphologies range between unweathered subrounded euhedral grains to subangular grains with slight to advanced degrees of surface corrosion.

4.5 | Q-F-Lt Petrography

Clast analysis of Cretaceous sediments is based on the two classification schemes devised by Dickinson et al. (1983), Qm-F-Lt plot (Figure 12A) and Qt-F-Lt plot (Figure 12B). Sandstones classify as subarkose, sublitharenite and quartz arenites. Petrographic observations show a transition from Early Cretaceous transitional continental to Late Cretaceous cratonic interior (Figure 12B). This transition trends from an arid to hot and humid paleoclimate as described by Suttner and Dutta (1986) and Weltje (1994).

4.6 | Zircon U/Pb Geochronology

Well TB-1 (Figure 13) zircons are predominantly Proterozoic in age; the proportion of Neoproterozoic zircons decrease from the Aptian to the Campanian, conversely the proportion of Paleoproterozoic zircons increase through time. Palaeozoic

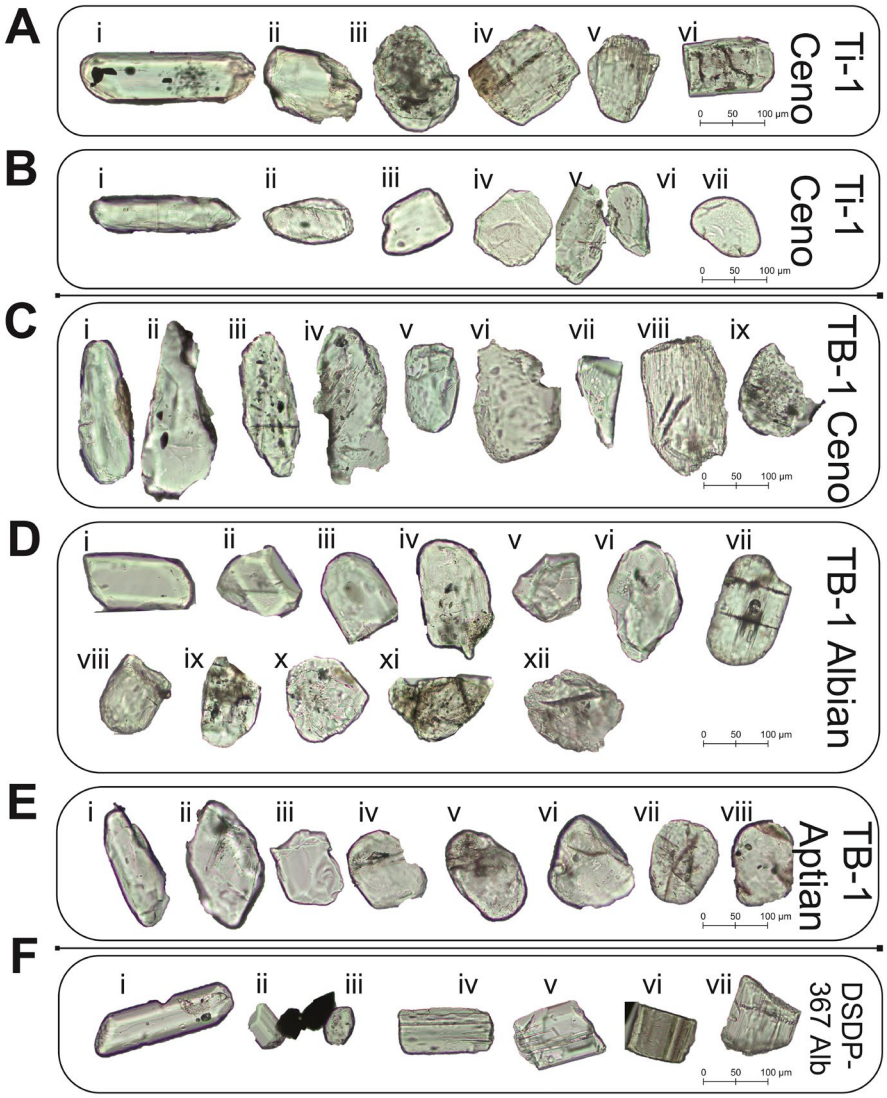

FIGURE 10 | Representative photomicrograph images of apatite observed under plain-polarised light. (A) Cenomanian, well Ti-1 (low ATi ratio), (i) subrounded euhedral grain, (ii–vi) subrounded to sub angular grains with initial to slight degrees of surface corrosion. (B) Cenomanian, well Ti-1 (high ATi ratio), (i) subrounded euhedral grain, (ii–vi) subrounded low-sphericity grains with surface conchoidal fracturing, (vii) rounded medium-sphericity grain with surface conchoidal fracturing. (C) Cenomanian, well TB-1, (i–ii) unweathered subangular low-sphericity grains, (iii–ix) initial to slight degree of surface corrosion. (D) Albian, well TB-1, (i–iv) subrounded subhedral grains, (v–xi) grains displaying initial surface corrosion, (xii) slight to advanced surface corrosion. (E) Aptian, well TB-1, (i–ii) subrounded euhedral grain, (iii–vii) rounded medium-sphericity grains. (F) Albian, DSDP 367, (i–ii) subrounded subhedral grain, (iii) subangular medium-sphericity grains with pitted surface etching, (iv–vi) angular grains with initial to slight corrosion, (vii) angular grain with advanced corrosion.

zircons are predominantly Carboniferous and Permian and are principally found within Aptian and Albian sediments of wells TB-1 and Nd-1. The proportion of Archean zircons increase throughout the Cretaceous with the highest proportion of Archean ages found within the Maastrichtian sediments of well Nd-1.

Zircon geochronology of sediments from Nd-1 (Figure 13) also exhibits a high proportion of Proterozoic ages with an increasing proportion of Meso-Paleoproterozoic zircons towards the Late Cretaceous. A significant quantity of zircons (23%) from Albian sediments are of CAMP age (*ca*. 200 Ma) with a far lesser contribution within the Aptian and Cenomanian sediments. Maastrichtian sediments from Nd-1 show an increase in Archean zircons similar to the Late Cretaceous sediments of TB-1. These Maastrichtian sediments also include a significant proportion of Cambrian zircons (20%).

Silurian sediments sampled from well DM-1 contain zircons predominantly Proterozoic in age, with a smaller population of Neo-Archean zircons. Wells DSDP 367, Br-1 and NCF-1 sediments contain proportionally similar populations of zircons, predominantly Proterozoic with a minor proportion of Archean and Palaeozoic ages. The sampled Maastrichtian sandstones from the Cap de Naze outcrop and well Nd-1 have similar zircon populations, with a significant proportion of Cambrian zircons (11%) and a lower proportion of Archean zircons. Cambrian zircons from Maastrichtian sediments of Nd-1 and Cap de Naze are diverse with ages ranging between 497 and 528 Ma.

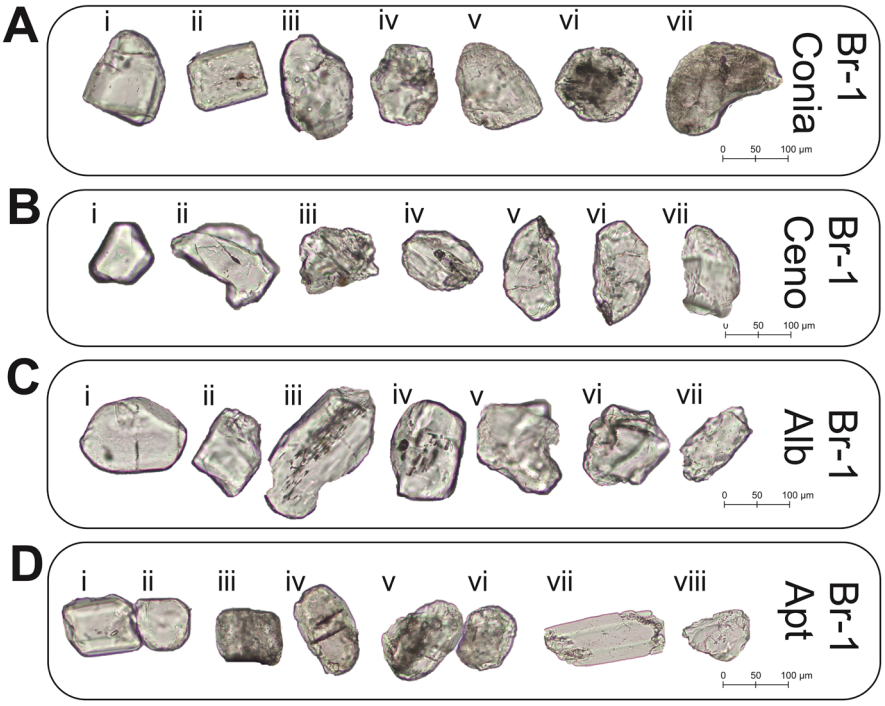

FIGURE 11 | Representative photomicrograph images of apatite observed under plain-polarised light. (A) Coniacian, well Br-1, (i) unweathered subrounded subhedral grain, (ii) subangular grain with initial stages of surface corrosion, (iii–vii) subrounded grains with initial to slight degrees of surface corrosion. (B) Cenomanian, well Br-1, (i) unweathered subrounded euhedral grain, (ii–vii) subrounded to subangular grains with initial to slight degrees of surface corrosion. (C) Albian, well Br-1, (i) unweathered subrounded subhedral grain, (ii–iv) subrounded grains with initial to slight degrees of surface corrosion, (v–vii) subangular grains with slight to advanced degrees of surface corrosion. (D) Aptian, well Br-1, (i–ii) unweathered subrounded grains, (iii–vi) subrounded grains with slight to advanced degrees of surface corrosion, (vii–viii) subangular moderately etched grains.

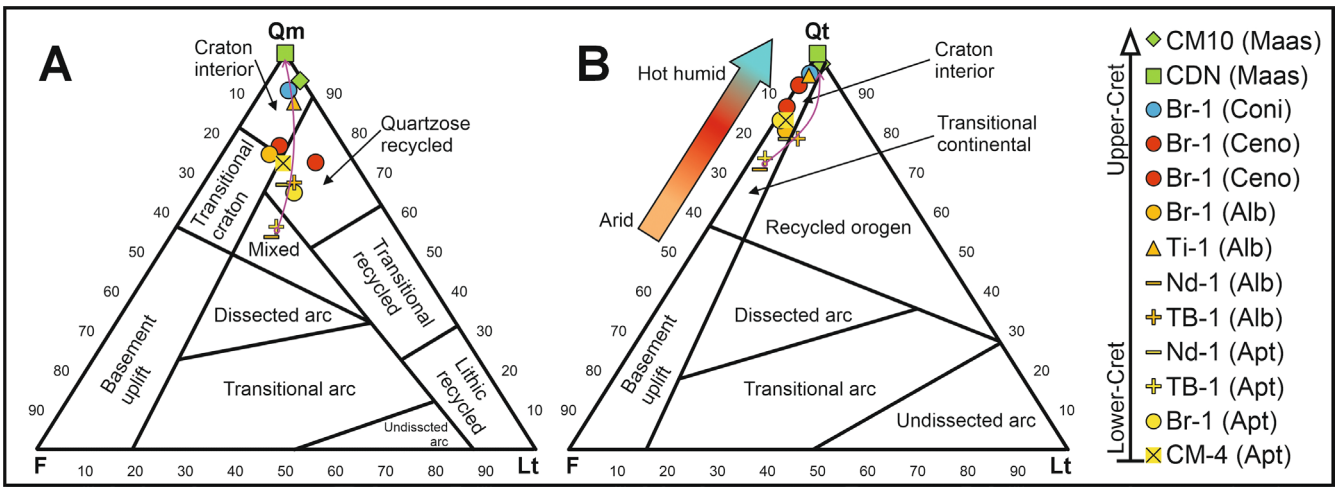

FIGURE 12 | (A) Qm-F-Lt plot; monocrystalline-quartz, feldspar (total) and lithic (igneous, metamorphic and sedimentary plus polycrystalline-quartz) and (B) Qt-F-Lt plot; quartz (total), feldspar (total) and lithic (igneous, metamorphic and sedimentary).

5 | Discussion

5.1 | Provenance, Diagenesis and Recycling

Diagenetic removal of detrital heavy minerals is restricted to the less-stable amphibole and pyroxene due to their occurrence is the Maastrichtian sands of Cap de Naze and Cap Rouge (Figure 4) but their absence from older basinal sediments. With limited diagenesis occurring at depth, textural variations of garnet from within the same sand-unit is more likely to be diagnostic of source, indicative of first cycle and recycled source lithologies. Garnets with significant cuboidal etching are recycled from Palaeozoic sandstones, whilst grains with minimal surface etching are directly sourced from first-cycle sources. Albian DSDP 367 garnets represent the oldest garnets which do not exhibit extensive cuboidal etching, the predicted source of these garnets is the KKI which is known to be a source of metasomatic grossular garnets (Mounteney

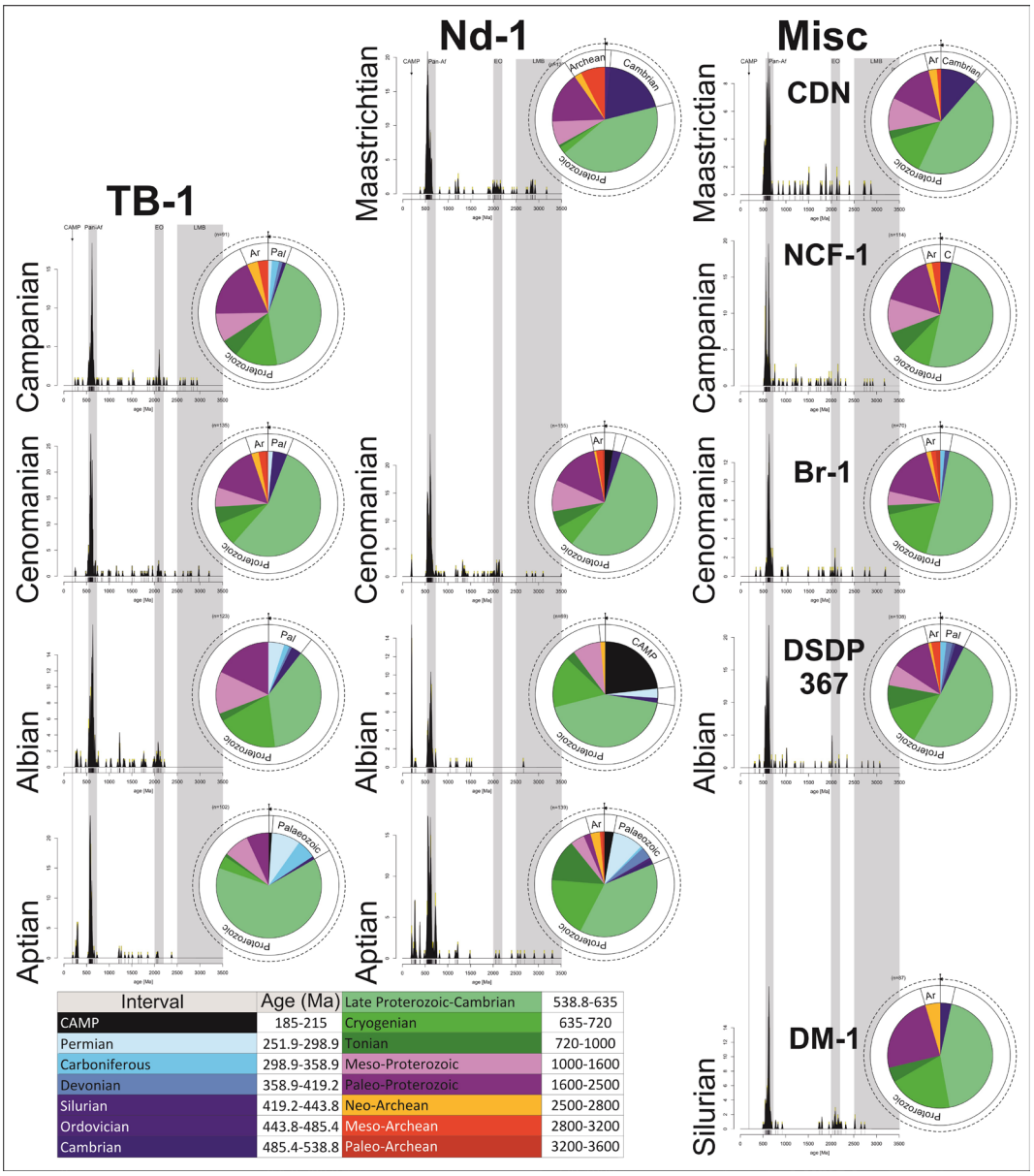

FIGURE 13 | Kernal density estimate (KDE) and corresponding pie-charts for U/Pb geochronology of detrital zircon from TB-1, Nd-1 and miscellaneous samples. Central Atlantic Magmatic Province (CAMP), Pan-African event (Pan-Af), Eburnean Orogeny (EO) and Leo-Man Basement (LMB).

et al. 2021). The lack of significant corrosion features is therefore likely to infer a first-cycle source. Aptian garnets from well TB-1 and Nd-1 are generally corroded with cuboidal etch facets except for a number of grains from TB-1 (Figure 8Dv–vii) which are blocky with low-degree of surface faceting. Albian garnet from well Nd-1 display the highest degree of corrosion with heavy cuboidal etching and skeletal remnants, these garnets are of Type-A high-grade metamorphic origin and Type-B igneous/metasedimentary source (Figure 7E), recycled from Palaeozoic sediments. Cenomanian garnets from wells TB-1 and Nd-1 both display dual morphologies and textures however, these features differ between the wells with TB-1 exhibiting cuboidal and 'microscaly' etching whilst Nd-1 garnets exhibit conchoidal fractured grains with slight surface corrosion and subrounded to rounded grains with slight surface corrosion. Speciation of garnet from both wells (Figure 7A,D) is indicative of an igneous/metasedimentary source for the garnets however, the mixed morphologies/textures indicate potential differences in recycled source rock and first-cycle igneous/metasedimentary source rocks; the similarity in garnet speciation between recycled and first-cycle sources is representative of facies replication. Santonian garnets (Figure 8A) from well TB-1 consist of rounded dodecahedral grains to blocky/fractured grains which are likely to have been sourced from continued erosion of a first-cycle igneous/metasedimentary lithology.

Aptian apatite's from wells TB-1 (Figure 10E) and Br-1 (Figure 11D) encompass a range in morphologies between subrounded with high sphericity and moderately etched subangular grains, indicating a degree of aeolian transportation, however, changes in the Early Cretaceous monsoonal climate developed

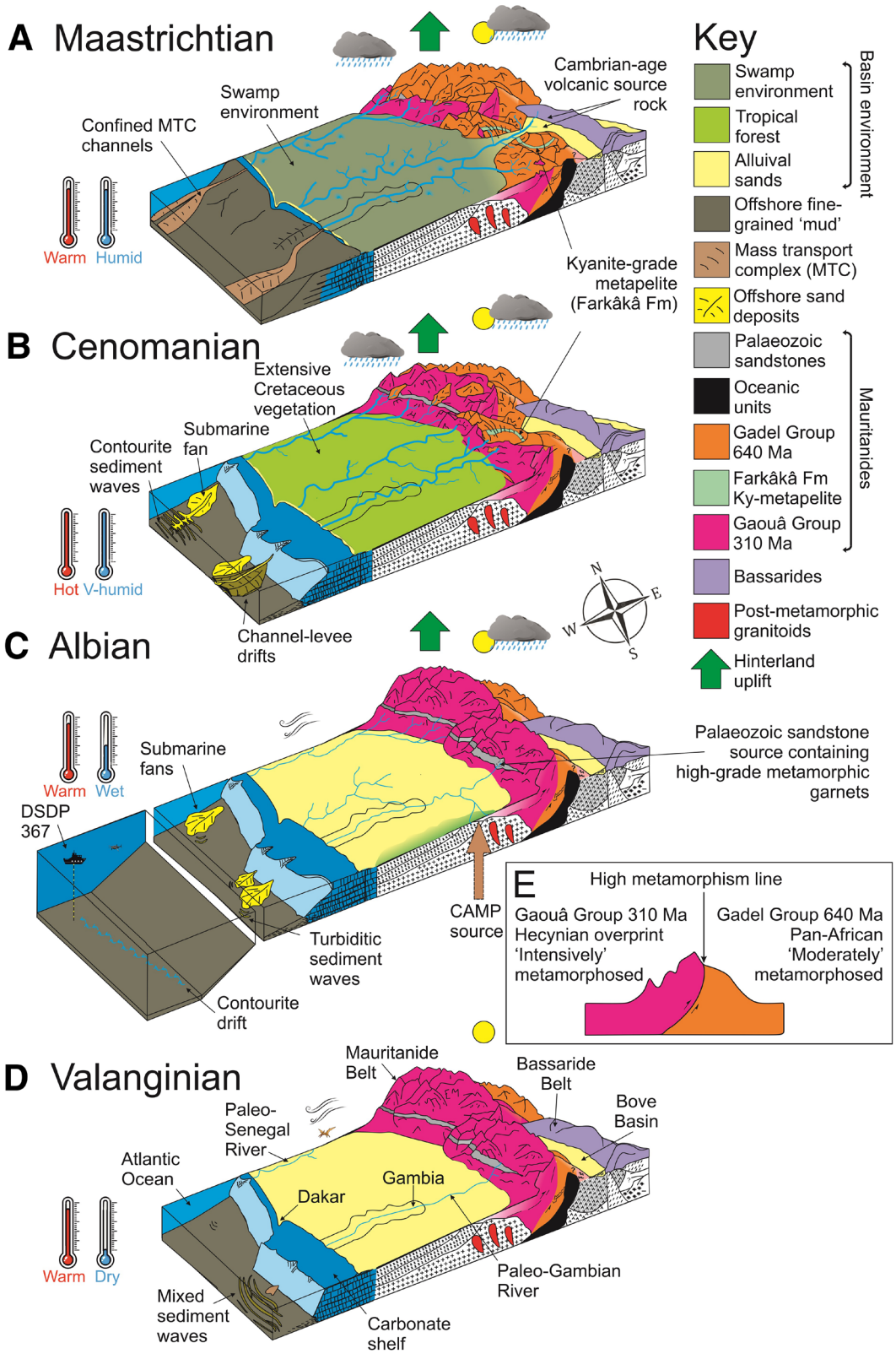

FIGURE 14 | Source to sink exhumation models for the Senegalese Basin, combining Cretaceous vegetation and climate evolution established from Pearson et al. (2023), orogenic uplift of the Mauritanides (Gouiza et al. 2019), exhumation and paleo-drainage evolution (this study). Subsurface structural geology adapted from Villeneuve (2008) and Caby and Kienast (2008). Figure not to scale in order to emphasise the denudation of the Mauritanides. (A) Maastrichtian. (B) Cenomanian. (C) Albian. (D) Valanginian. (E) Simplified cross section of the Mauritanides depicted in Figure 3 displaying the high metamorphism line described by Villeneuve (2008).

modest fluvial systems throughout the basin recycling intrabasinal sediments. Albian to Cenomanian onshore basin apatite's from well TB-1 range in morphology from subrounded euhedral to subrounded-angular, with initial degrees of surface corrosion indicative of limited alluvial-stage chemical weathering. However, Albian apatite's from DSDP 367 (Figure 10F) exhibit subrounded euhedral prismatic grains to angular grains with initial to slight corrosion which are principally fluvial in origin.

The similarity in provenance between wells Ti-1 and Br-1 (Figures 4 and 5) infers a common detrital source, although variation in ATi values (Figure 6) between the wells Ti-1 and Br-1 vary considerably. Exploration well Ti-1 is located inland approximately 90 km east of Dakar, associated ATi values (Figure 6B) include two distinct populations represented by high ATi and low ATi values. Typically, lower ATi values are diagnostic of extensive subaerial weathering of apatite during the alluvial stage (Figure 10A), however, the degree of apatite surface corrosion for Cenomanian sediments with higher ATi values (Figure 10B) is initial-slight suggesting the degree of alluvial-stage weathering is insufficient to cause the low ATi values (Figure 6B). Indeed, the lowest ATi values for Ti-1 Cenomanian sediments represent the youngest of the analysed Ti-1 sediments with the decrease in apatite content reflecting the basin-wide shift in sediment provenance as observed in well TB-1. The single low ATi Albian sediment (Figure 6B) is stratigraphically in the midpoint (Figure 4) of the higher ATi Albian sediments and is likely due to exceptional hydraulic sorting of the sediment. Whilst subtle, the differences in apatite surface corrosion for sediments with varying ATi values are still indicative of variations in alluvial-stage weathering that would be indicative of different depositional environments including riverbed-load environment (Figure 10B) and a point-bar environment (Figure 10A). These variations in corrosion textures are therefore representative of a transitional-wandering or multi-thread braided system with several branching channels (Rinaldi et al. 2016).

Exploration well Br-1 is located close to the modern-day coastline of Senegal (Figure 1B), associated intermediate ATi values are grouped as a single cluster (Figure 6C). Several explanations can account for variable ATi values in sedimentary systems, including hydraulic sorting, changes in source area, mechanical instability during transportation and post-depositional dissolution (Morton 1986). Apatite corrosion textures range from initial to advanced, however, final corrosive stages represented by skeletal morphologies are absent from the entirety of the Br-1 sediments suggesting alluvial-stage dissolution occurred, but not sufficiently enough to reduce the apatite content as a whole.

Observations of apatite and garnet textures negate the probability that alluvial-stage weathering and diagenesis had any measurable effect on heavy mineral content. As differences in detrital heavy mineral provenance are not the result of diagenesis by interstratal dissolution, they are therefore an accurate representation of changes in sediment source through the lateral unroofing of the Mauritanide Belt.

Deciphering tectonic and metamorphic characteristics of the Mauritanides can be locally complicated (Villeneuve 2008); predicting sediment source can be equally difficult when significant unroofing has occurred, completely eroding source terranes which no longer exist in modern geology. However, generalised metamorphic trends along the axis of the Mauritanides have been identified with 'advanced' metamorphism on the westward side containing the Gaouâ Group and 'moderately' metamorphosed suites on the eastern side containing the Gadel Group (Figure 14; Caby and Kienast 2008). The 'intensively' metamorphosed terrane of the western flank of the Mauritanides represent the first stage of active exhumation during the Early-mid Cretaceous characterised by the significant increase in garnet content (Figure 14C). Occurrences of high-grade metamorphic garnets which observed in Early Cretaceous sediments (Figure 7C,E) are heavily corroded and likely recycled from Palaeozoic sandstones within the Gaouâ Group. Significant exhumation of the Mauritanides continued throughout the mid-late Cretaceous as response to the changes in climate to hothouse conditions and uplift of the hinterland, resulting in the lateral shift in sedimentary source to the eastward side of the high metamorphism line (Figure 14B). This change in source to a 'moderately' metamorphosed terrane is characterised by staurolitic-grade basinal sediments (Figure 4). However, the occurrence of kyanite in well Nd-1 but not TB-1 suggests a different grade metamorphic source rock for the northern and southern Mauritanides with a higher-grade kyanite-bearing metapelites to the south (Figure 14A,B; Farkâkâ Formation). Garnet is present throughout the entirety of well Nd-1 and only becomes absent in well TB-1 during the Campanian, it is likely that garnet is still being sourced from the Mauritanides throughout the latter stages of the Cretaceous. This absence of garnet may be attributed to either a punctuated shift in metasedimentary source which is devoid of garnet or there has been a degree of hydraulic sorting during the transportation stage, preferentially removing the garnet from the Campanian sediments of TB-1.

Aptian to Albian sediments contain a significant proportion of Carboniferous to Permian zircon reflecting the primary stages of lateral unroofing of the Gaouâ Group source lithologies, representative of Hercynian thermal overprinting. The inclusion of Proterozoic Pan-African zircons within the Gaouâ Group represents recycling of Palaeozoic sandstones and core isotopic crystallisation ages associated with Pan-African I and II events.

Zircon geochronological trends for wells Tb-1 and Nd-1 correspond with shifts in detrital heavy mineral assemblages through apatite-garnet-staurolitic bearing sediments (Figures 4 and 13). Aptian sediments of wells TB-1 and Nd-1 are dominated by Neoproterozoic zircons which decreases throughout the Cretaceous with corresponding increases in Meso-Paleoproterozoic and Archean zircons. This trend in zircon geochronology reaffirms the model for lateral unroofing of the Mauritanide Belt throughout the mid-late Cretaceous. The timing for this unroofing event is synchronous with the unroofing of the White Mountains, a subrange of the Appalachian Belt which is believed to have accelerated during the Albian (Roden-Tice, Eusden-Jr, and Wintsch 2012) as a consequence to global climate change.

Two distinct changes in zircon provenance occur within the Albian sediments of Nd-1 and Maastrichtian sediments of Nd-1 and Cap de Naze. Albian sediment include a high proportion of CAMP zircons. Known sources of CAMP volcanics

within close proximity of Senegal include the lowermost limit of the Tioujdal Group to the east of the Mauritanide Belt and high-Ti Group CAMP lavas throughout Sierra Leone and Liberia (Marzoli et al. 1999, 2018). The Tioujdal Group volcanics are an unlikely source for these Albian sourced CAMP zircons, as the Mauritanide Belt would have been a geographic barrier preventing fluvial capture of this terrane. The northern limit of the High-Ti Group CAMP lavas in Sierra Leone may also be too distal to be a source. However, the present day distribution of these lavas may not represent their full extent during the Early Cretaceous, which may have cropped out further north within the region that hosts the Fouta Djallon Sills (Figure 15). The lack of modern-day evidence for extension of High-Ti Group CAMP lavas as far north as the FDP may be due to either burial beneath Mesozoic-Cenozoic sediments and/or near-complete erosion during the Cretaceous. A small number of CAMP zircons are still recorded during the Cenomanian, which could infer partial recycling of Albian sediments, a reduced fluvial catchment within the FDP or near-complete erosion of CAMP lavas during the Albian, therefore reducing the availability of a CAMP source in the Cenomanian. Another possible source for these CAMP zircons is through the surface manifestation of a tholeiitic volcanic dome structure located at the total depth of Nd-1 (3458 m; Ndiaye et al. 2016), although this would not account for the significant shift in garnet source encountered within the Albian sediments (Figure 7E).

Maastrichtian sands from Cap de Naze and Nd-1 contain a significant proportion of Cambrian zircons (Figure 8). The closest proximal source for these zircons are the Early Cambrian Nagara and Bouly Group volcanics and Late Cambrian Nandoumba Group intrusive basalts located in the southern extent of the Bassarides (Villeneuve et al. 2014). It is unknown if these Cambrian zircons are sourced directly from the Bassarides or recycled from the Bove Basin Palaeozoic sediments located between the southern Mauritanides and Bassarides (Figures 1C, 14 and 15). For the paleo-Saloum catchment to include these Cambrian volcanics, significant pre-Maastrichtian erosion of the southern Mauritanides must have occurred, allowing for the addition of this Cambrian-sourced detritus. The diverse range in Cambrian age (497–538 Ma) zircons may reflect a combination of these sources, however, an unknown proportion of Early Cambrian zircons may also be representative of late-stage Pan-African II overprinting with recorded ages for this event ranging between 635 and 520 Ma (Villeneuve et al. 2014) with a temporal overlap of *ca*. 18 Ma. The paleo-Senegal River isn't predicted to source sediment from within the region of the Early Cambrian Nagara and Bouly Group volcanics or the late Cambrian Nandoumba Group intrusive basalts, therefore Maastrichtian sediments from well TB-1 would be extremely useful in precisely constraining late-stage Pan-African II overprinting of the Mauritanide Belt which was exposed during the Maastrichtian, unfortunately to our knowledge they do not exist.

5.2 | Paleo-Drainage

Varietal heavy mineral provenance of basin sediments implies at least three potential major paleo-drainage systems within the Senegal Basin. The geometry of these paleo-river systems is comparable to their modern-day counterparts, suggesting these systems are long-lived. However, changes in temporal sedimentary provenance suggests varying degrees of catchment evolution throughout the Cretaceous occurring during periods of significant climate change. Combining the interpretation of provenance and climate evolution (Pearson et al. 2023), it is possible to predict paleo-drainage throughout the Senegal Basin during the Cretaceous (Figure 15). Climate, subsurface-geology, topography and vegetation all control fundamental aspects of river geometry; of these four aspects, topography can be the hardest to predict through multiple orogenic cycles, dynamic uplift and erosion. The reconstruction of paleo-elevation in eroded orogens has been calculated using various methods (Mulch et al. 2004; Hu et al. 2020; Hillenbrand and Williams 2021). Unfortunately, no such data exists for the orogenic terranes of NW Africa, therefore the predicted paleo-elevation of the Mauritanides is based on inferences from similar orogenic terranes.

The Mauritanide Orogeny is associated with the larger Appalachian Orogeny during the Late Permian (Figure 2A). Predicted paleo-elevation of the Appalachians are in the range of 5–7 km with crustal thickness estimations of 55–70 km (Hillenbrand and Williams 2021). If Airy-type isostatic balance is assumed, the correlation between crustal thickness and topography can be used to estimate the paleo-elevation of the Mauritanides during the Mesozoic (Beck et al. 1996). Calculated crustal thickness of the Mauritanides is between 32 and 34 km (Globig et al. 2016), half the thickness of the Appalachian crust; suggesting a maximum paleo-elevation for the Mauritanides of 2.5–3.5 km during the Mesozoic. The residual mountain widths of the Mauritanides range from *ca*. 150 km for the northern segment to *ca*. 50 km for the southern segment, inferring a higher paleo-elevation for the northern segment of the Mauritanides. It is more difficult to predict the paleo-elevation of the Bassarides because they were formed during a much older orogenic event (Figure 2B) but was likely to have been higher than today. The modern-day Senegal River's catchment is still governed by the current elevation of the Mauritanides despite its comparatively low relief, with maximum elevations of ~150 m ASL (Figure 1A). The Senegal River breaches the Mauritanides between Bakel (Senegal; N14°54′) and Keyes (Mali; N14°27′) where its catchment expands into the Taoudeni Basin, KKI and the northern limits of the Leo-Man Shield.

5.3 | Paleo-Senegal River

Offshore submarine siliciclastic fans off the coast of northern Senegal, adjacent to the exploration well of TB-1 (Figure 14B–D) exist throughout the Aptian and Cenomanian/Turonian. The river mouth for these offshore deposits is similar to the exit of the modern-day Senegal River, suggesting the river geometry has changed very little throughout the previous *ca*. 125 Ma. Therefore, the antecedent drainage geometry of this river is postulated to be governed via deep-seated subsurface structures. The east–west nature of the Senegal River is parallel to that of the Gambia River suggesting an association with the rift grabens which strike into the continent. Paleo-Senegal River morphology is likely to range between sinuous and meandering-unconfined

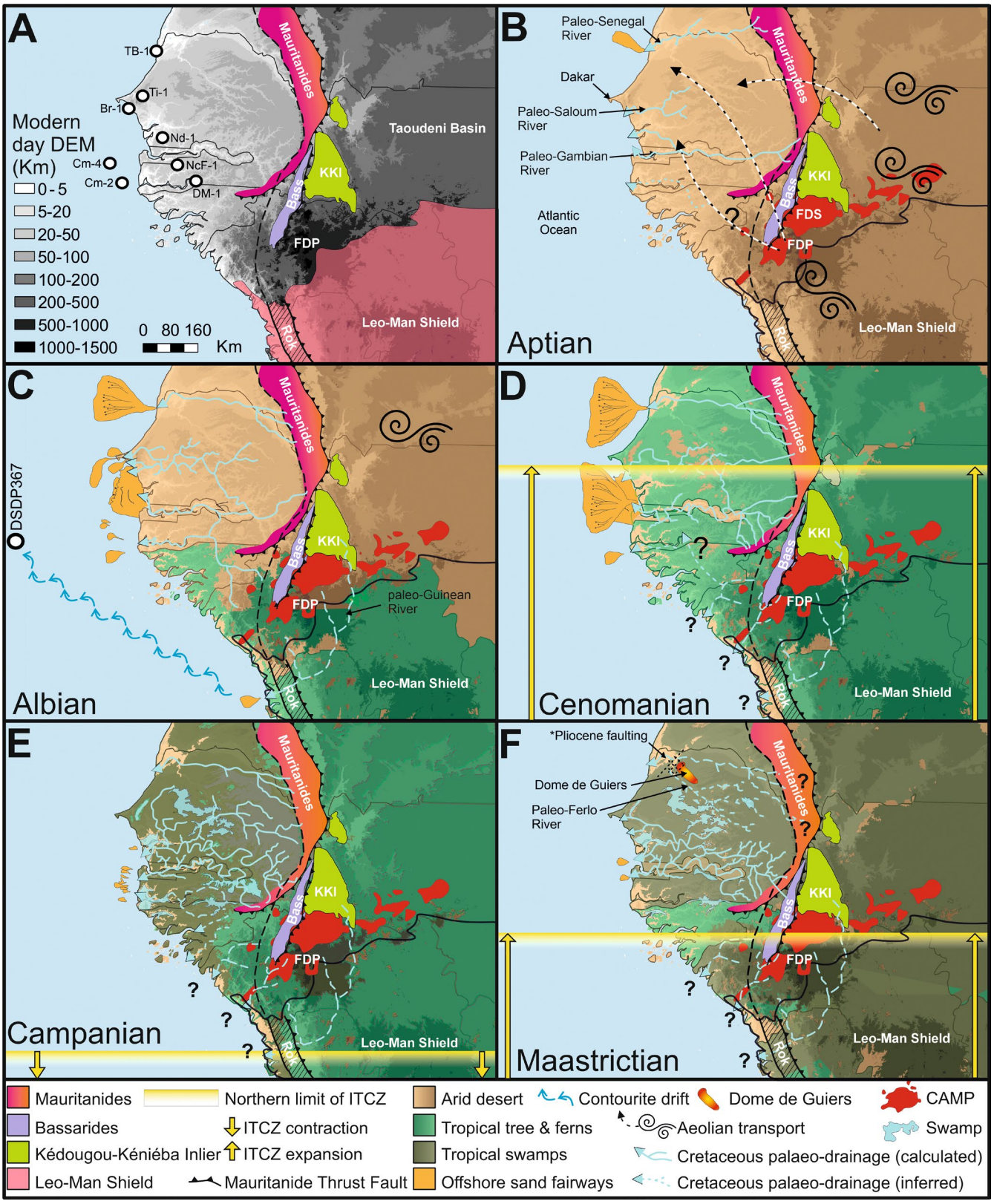

FIGURE 15 | Paleo-drainage reconstructions of Senegal throughout the Cretaceous. (A) Modern-day DEM with superimposed potential source terranes. (B) Aptian. (C) Albian. (D) Cenomanian. (E) Campanian and (F) Maastrichtian. Bassarides (Bas), Fouta Djallon Sills (FDS), Fouta Djallon Plateau (FDP), Kedougou-Kenieba Inlier (KKI), Intertropical Convergence Zone (ITCZ), Central Atlantic Magmatic Province (CAMP), Dome de Guiers (DdG).

single-thread, similar to the meandering nature of the modern-day Senegal River (Sadio et al. 2017). The lack of divergence in the paleo-Senegal River suggests the river maintained a fast-flowing velocity throughout the mid-late Cretaceous, which would be crucial in the transportation of large volumes of sediment offshore. The provenance of these sediments exhibits an

unroofing event continuing beyond the Cretaceous with the drainage catchment restricted to the high-altitude northern Mauritanides. It is unclear as to when the paleo-Senegal river breached the northern Mauritanides allowing the erosion of Taoudeni Basin and KKI, due to a lack of Maastrichtian sedimentological data from the north. An increase in topographic elevation in northern Senegal, caused by the emplacement of the Dome de Guiers (Trenous and Michel 1971), may have redirected drainage from the basin northwards and into the paleo-Senegal River, resulting in the formation of the proto-Ferlo River. Prolonged inflation of the dome throughout the Pliocene would eventually cause orthogonal faulting of the region, permanently controlling the geometry of the modern-day Ferlo River and resulting in the creation of Lake de Guiers (Figure 14F).

5.4 | Paleo-Saloum River

The paleo-Saloum, like its modern-day counterpart, was probably the smallest of the Senegalese rivers. Restricted to recycling pre-Cretaceous sediment from the onshore basin interior during the Early Cretaceous. The river only began to erode the Mauritanides during the Cenomanian as evidenced by the inclusion of garnets from the 'intensively' metamorphosed western flank of the Mauritanide Belt into the basin sediments. The system is likely to have a common source to the Paleo-Gambia River during the Late Cretaceous due to the inclusion of kyanite-grade metapelite source rocks and the inclusion of Cambrian zircons predicted to have been sourced from the Bassarides and/or Bove Basin.

5.5 | Paleo-Gambia River

This river is known to have existed prior to the Cretaceous period (Long and Cameron 2016; Casson 2020). The Gambia River is confined within the region of the Casamance failed rift arm, associated with the existence of subsurface grabens between 50 and 100 km wide striking up to 400 km into the continent (Burke 1976). These structures are postulated to control the antecedent drainage of the proto-Gambia River (Long and Cameron 2016; Casson 2020). It is therefore plausible that the Cretaceous paleo-Gambia River resided within the same region as the modern-day river. Sedimentary data for the paleo-Gambia system is based upon data from Nd-1. Sedimentary provenance suggests erosion of basinal sediments during drier seasons with erosion of the central-southern Mauritanides during wetter seasons. Temperature and humidity increased during the Albian as a result of the expanding paleo-ITCZ, elevated levels of precipitation were concentrated over upland regions of southern NW Africa to include Leo-Man Shield and FDP. Increased precipitation in southern-upland NW Africa diverted the catchment of the paleo-Gambia River southwards to capture detritus from within the FDP sourcing CAMP zircons from Fouta Djallon volcanics. Further expansion of the paleo-ITCZ during the Late Cretaceous increased precipitation northwards rediverting the paleo-Gambia catchment back towards the lower Mauritanides.

It is unclear if drainage of the FDP continued into the Senegal Basin during the Late Cretaceous due to a lack of CAMP zircons; although it is possible that these source rocks were exhausted during the Albian exhumation. The source catchment of the paleo-Gambia River remained relatively static throughout the remainder of the Cretaceous unroofing the southern Mauritanides until sufficient denudation had occurred to allow expansion of the river catchment into the southern Bassarides. These observations demonstrate a divergent fluvial system throughout the basin with multiple channel bars creating a braided-fluvial system throughout the basin (Figure 15E,F).

5.6 | Paleo-Casamance River

The fourth modern-day Senegalese river is the Casamance located south of Gambia, unfortunately there is insufficient data to conclusively support the evidence for a southern system analogous to the Casamance.

5.7 | Paleo-Guinean River

Evidence of a paleo-Guinean fluvial system is speculative and based on evidence from a single sample of Albian sand from well DSDP 367. Whilst a single sample is not entirely diagnostic of an additional system, the unique provenance of this sediment cannot be ignored. Cretaceous elevation of the Mauritanides prevents direct sourcing of KKI detritus into the proto-North Atlantic via Senegal, as evidenced by the lack of the Type Ci and D garnets within the Cretaceous onshore basinal sediments. However, a southern Guinean system bypassing the Mauritanides could have an erosional catchment encompassing the KKI, FDP and Bove Basin. This fluvial system would have to flow north to south before turning to deposit sediment offshore to the west (Figure 15C). Contourite currents are the likely transport mechanism offshore moving the sands along strike, parallel to the shelf margin and then in the deep basin (Figures 14C and 15C). Palaeoceanographic currents during the Early Cretaceous are interpreted to flow south to north (Hay 2009) along the NWAAM, with evidence of extensive contourite deposits recorded on 3D seismic onshore in the shelf slope and basin by (Coskun et al. 2023). One problem with this model is the absence of any CAMP zircons in DSDP 367, which are abundant in Albian sediments in well Nd-1 (Figure 8) and are assumed to be derived from the FDP. The lack of CAMP zircons in Albian sands from DSDP 367 does not preclude a source from part of the FDP, as the exact extent of exposed CAMP volcanics during the Cretaceous is unknown.

6 | Conclusion

Mineralogical analysis of Cretaceous sediments from Senegal records several shifts in provenance; these shifts are interpreted to reflect a dominant climate control and the evolution to a hotter and more humid environment. As temperature and humidity increased throughout the Cretaceous, so did precipitation and denudation of the Mauritanide Belt. This was exacerbated further through the dynamic uplift of the hinterland, increasing sediment supply into the Senegalese onshore and offshore basins.

Cretaceous paleo-drainage maintains a strong resemblance to the modern-day drainage of the Senegal Basin with two major fluvial systems; the paleo-Senegal and paleo-Gambia, and a comparatively minor fluvial system akin to the modern-day Saloum. No provenance data exists for the Casamance region of Senegal, but fluvial systems are highly likely due to the proximity of the high-altitude FDP. The paleo-Gambia river is a long-lived system that may have existed as far back as the Jurassic as a consequence of the Casamance failed rift arm. The paleo-Senegal river is also a long-lived system existing since at least the Cretaceous, flowing east to west the river is parallel to the subsurface grabens which strike hundreds of kilometres into the continent as a result of the Atlantic rifting. It is unclear if the paleo-Saloum is controlled via subsurface structures or just the result of alluvial-type drainage across a broad flat basin.

Whilst the modern-day rivers and their Cretaceous counterparts share distinct similarities, the most significant difference between the two source to sink systems are the paleo-elevation of the Mauritanides. Maximum estimated paleo-elevation for the northern segment of the Mauritanides is 2.5–3.5 km, based upon the crustal thickness comparison between the Appalachian and Mauritanide orogenic belts. It is unknown to what degree the Mauritanides may have been eroded throughout the Triassic and Jurassic, however, Cretaceous paleo-elevation is assumed to be greater than today restricting paleo-river catchments to the windward side of the Mauritanides. Dynamic uplift of up to 2 km for the Mauritanides is calculated from low-temperature thermochronology between the Albian and Maastrichtian; this uplift exacerbated orogenic denudation whilst maintaining a geographical barrier for most of the Cretaceous between the Senegal Basin and the surrounding hinterland.

During the very Early Cretaceous (Berriasian–Barremian) NW Africa was principally arid with limited geostrophic precipitation, any fluvial systems existing during this period would have been minor, seasonal and restricted to the basin interior.

Continued fragmentation of Gondwana during the Early Cretaceous caused the disruption of the large low-pressure cell which existed during the summer in the southern hemisphere, resulting in the expansion of the equatorial tropics. Expansion of the equatorial tropic zone increased precipitation in highland regions of southern NW Africa including the FDP and Leo-Man Shield. This increased precipitation expanded the paleo-river catchments; the Senegal expanded eastwards, continuing to erode the northern Mauritanides and the paleo-Saloum expanded within the basin, continuing to recycle pre-Cretaceous basinal sediments. The paleo-Gambia system which was previously eroding the southern extent of the Mauritanides during the Aptian, diverted southwards sourcing sediment from the FDP highlands, evidenced by high-grade metamorphic garnets and CAMP detrital zircons.

Climate change accelerated during the Cenomanian and Turonian, entering into the CTM-hothouse period. Temperature, humidity and precipitation reached a Cretaceous high during this period, significantly increasing denudation of the Mauritanides, delivering large volumes of sediment offshore as extensive submarine fan deposits. During this period, the paleo-Senegal and paleo-Saloum rivers continued to erode the northern segment of the Mauritanides through fluvial incision of the orogenic terrane and lateral unroofing of the 'intensively' metamorphosed domain followed by the successive erosion of the 'moderate' metamorphic domain on the eastern flank of the Mauritanides. Cessation of the CTM occurred during the Coniacian returning global climate to a Cretaceous 'norm' of a warm and humid environment. Paleo-drainage remained unchanged during this interval; however, environmental and ecological conditions began to evolve throughout the basin gradually transitioning into a swamp-like environment. By the Maastrichtian aquatic fern-spores collected from Senegalese sediments verify hot and damp ecological conditions with extensive vegetation found around lakes and swamps. This transitional environment restricted clastic sedimentation to the onshore basin, whilst offshore sediment deposition was predominantly in the form of fine-grained MTC's with small-scale siliciclastic deltas prograding from the continental shelf. Although no Maastrichtian provenance data exists for the paleo-Senegal river it is assumed to have continued to erode the northern Mauritanides given the rivers longevity and the continued humid-climate of the Late Cretaceous. Uplift of Dome de Guiers in northern Senegal during the Maastrichtian may have begun to divert northern paleo-drainage towards the paleo-Senegal River forming the proto-Ferlo River. Central paleo-Saloum and paleo-Gambia rivers which has been sourcing sediment from the southern Mauritanides throughout much of the Cretaceous began to breach this orogenic belt; allowing the expansion of these rivers to capture the catchment of the southern Bassarides, as evidenced by the occurrence of Cambrian volcanic zircons in Nd-1 and Cap de Naze Maastrichtian sediments.

This research demonstrates the long-established nature of the Senegalese river systems, which were pivotal in the delivery of sediment into the MSGBC Basin throughout the Cretaceous. Paleo-river catchments were restricted to the basin interior initially recycling pre-Cretaceous basinal sediments until climate change increased the fluvial incision and lateral W–E exhumation of the Mauritanides. Cretaceous basinal sediments consist of recycled pre-Cretaceous sediments, Palaeozoic sandstones consisting of detritus associated with the erosion of the West African Pan-African orogenic belts and varying-grade metamorphic source rocks linked to the Hercynian Orogenic event.

Acknowledgements

This study marks the concluding stage of the lead authors PhD project at the University of Manchester. We thank the sponsoring companies of the North African Research Group (NARG) for their continued financial and scientific support. Petrosen of Dakar, Senegal for access to their core and cuttings repository. Finally, thanks to the British Geological Survey for their support and analytical facilities. We also acknowledge the National Environmental Isotope Fund (NEIF) for this funding towards the zircon geochronology and William Tampion-Lacey for his help in the acquisition of the U/Pb geochronological isotopic data. We would also like to acknowledge the manuscript reviewers and thank them for their valuable input.

Conflicts of Interest

We wish to confirm that there are no known conflicts of interest associated with this publication and there has been no significant financial support for this work that could have influenced its outcome.

Data Availability Statement

The data that support the findings of this study are available from the corresponding author upon reasonable request.

References

Afanasiev, V. P., O. V. Snegirev, O. A. Kozmenko, and N. P. Pokhilenko. 2013. "Chemical Weathering of Kimberlitic Garnets: An Experimental Study (Organic Etching in ATP-Na_2 Salt)." *Geochemistry* 459: 1528–1532. https://doi.org/10.1134/S1028334X14120010.

Ando, S., E. Garzanti, M. Padoan, and M. Limonta. 2012. "Corrosion of Heavy Minerals During Weathering and Diagenesis: A Catalog for Optical Analysis." *Sedimentary Geology* 280: 165–178. https://doi.org/10.1016/j.sedgeo.2012.03.023.

Barusseau, J. P., J. Roger, B. J. Noel, O. Serrano, and C. Duvail. 2009. *Notice explicative de la carte géologique du Sénégal à 1/200 000, feuilles de Saint-Louis–Dagana, Podor–Saldé, Matam Semmé*. Dakar: Ministère des Mines, de l'Industrie et des PME, Direction des Mines et de la Géologie.

Beck, S. L., G. Zandt, S. C. Myers, T. C. Wallace, P. G. Silver, and L. Drake. 1996. "Crustal-Thickness Variations in the Central Andes." *Geology* 24, no. 5: 407–410. https://doi.org/10.1130/0091-7613(1996)024<0407:CTVITC>2.3.CO;2.

Bellion, Y., and G. Crevola. 1991. "Cretaceous and Cainozoic Magmatism of the Senegal Basin (West Africa): A Review." In *Magmatism in Extensional Structural Settings*, 189–208. Berlin, Heidelberg: Springer. https://doi.org/10.1007/978-3-642-73966-8_8.

Brownfield, M. E., and R. R. Charpentier. 2003. "Assessment of the Undiscovered Oil and Gas of the Senegal Province, Mauritania, Senegal, The Gambia, and Guinea-Bissau, Northwest Africa." US Geological Society Bulletin 2207-A. https://pubs.usgs.gov/bul/b2207-a/b2207-a.pdf.

Buchs, D. M., A. C. Kerr, J. C. Brims, J. P. Zapata-Villada, T. Correa-Restrepo, and G. Rodríguez. 2018. "Evidence for Subaerial Development of the Caribbean Oceanic Plateau in the Late Cretaceous and Paleo-Environmental Implications." *Earth and Planetary Science Letters* 499: 62–73. https://doi.org/10.1016/j.epsl.2018.07.020.

Burke, K. 1976. "Development of Graben as Sociated With the Initial Ruptures of the Atlantic Ocean." *Developments in Geotectonics* 12: 93–112. https://doi.org/10.1016/B978-0-444-41549-3.50011-6.

Caby, R., and J. R. Kienast. 2008. "Neoproterozoic and Hercynian Metamorphic Events in the Central Mauritanides: Implications for the Geodynamic Evolution of West Africa." *Journal of African Earth Sciences* 53: 122–136. https://doi.org/10.1016/j.jafrearsci.2008.09.004.

Caracciolo, L., S. Critelli, W. Cavazza, and G. Meinhold. 2014. "The Rhodope Zone as a Primary Sediment Source of the Southern Thrace Basin (NE Greece and NW Turkey): Evidence From Detrital Heavy Minerals and Implications for Central-Eastern Mediterranean Palaeogeography." *International Journal of Earth Sciences* 104: 815–832. https://doi.org/10.1007/s00531-014-1111-9.

Casson, M. 2020. "Tectono-Stratigraphic Evolution of the Mesozoic Continental Margins of the Central Atlantic." A Thesis Submitted to the University of Manchester, Chapter 6.

Casson, M., G. Calvès, M. Huuse, B. Sayers, and J. Redfern. 2020. "Cretaceous Continental Margin Evolution Revealed Using Quantitative Seismic Geomorphology, Offshore Northwest Africa." *Basin Research* 33, no. 1: 66–90. https://doi.org/10.1111/bre.12455.

Chamley, H., P. Debrabant, A.-M.Candillier, and J. Foulon. 1983. "13. Clay Mineralogical and Inorganic Geochemical Stratigraphy of Blake-Bahama Basin since the Callovian, Site 534, Deep Sea Drilling Project Leg 761." *Init Repts DSDP* 76: 437–451. https://doi.org/10.2973/DSDP.PROC.76.113.1983.

Chamley, H., P. Debrabant, and R. Flicoteaux. 1988. "Comparative Evolution of the Senegal and Eastern Central Atlantic Basins, From Mineralogical and Geochemical Investigations." *Sedimentology* 35: 85–103.

Coskun, S. D., G. Calves, I. Kane, M. Huuse, and J. Redfern. 2023. "Sediment waves as a tool to understand deep-water current evolution, Senegal Basin, NW Africa." Paper presented at the 4th Deep Water Circulation Research Conference, Edinburgh, UK, May.

Davison, I. 2005. "Central Atlantic Margin Basins of North West Africa: Geology and Hydrocarbon Potential (Morocco to Guinea)." *Journal of African Earth Sciences* 43, no. 1–3: 254–274. https://doi.org/10.1016/j.jafrearsci.2005.07.018.

Decker, J., K. Helmold, R. Ingersoll, T. Bullard, R. Ford, and J. Pickle. 1985. "The Effect of Grain Size on Detrital Modes; a Test of the Gazzi-Dickinson Point-Counting Method; Discussion and Reply." *Journal of Sedimentary Research* 55: 618–621. https://doi.org/10.1306/212F878D-2B24-11D7-8648000102C1865D.

Dia, O. 1984. "La chaıne panafricaine et hercynienne des Mauritanides face au bassin Proterozoıque superieur a Devonien de Taoudeni, dans le secteur clef de Mejeria (Taganet, sud RIM)." These dEtat, Universite Aix–Marseille III, Marseille.

Dickinson, W. R., L. S. Beard, G. R. Brakenridge, et al. 1983. "Provenance of North American Phanerozoic Sandstones in Relation to Tectonic Setting." *Geological Society of America Bulletin* 94, no. 2: 222–235. https://doi.org/10.1130/0016-7606(1983)94<222:PONAPS>2.0.CO;2.

Dou, L., X. Zhang, K. Xiao, et al. 2023. "Early Cretaceous (Aptian to Albian) Vegetation and Climate Change in Central Africa: Novel Palynological Evidence From the Doseo Basin." *Geological Journal* 59, no. 2: 441–467. https://doi.org/10.1002/gj.4873.

Effimoff, I., and J. Keall. 2018. "Extended Abstract: SNE and FAN World Class Discoveries Offshore Senegal Herald a Major New Hydrocarbon Province." *Houston Geological Society Bulletin* 61, no. 2: 12.

Evenick, J. C. 2021. "Glimpses Into Earth's History Using a Revised Global Sedimentary Basin Map." *Earth-Science Reviews* 215. https://doi.org/10.1016/j.earscirev.2021.103564.

Farrant, A. R., I. Mounteney, A. Burton, et al. 2018. "Gone With the Wind: Dune Provenance and Sediment Recycling in the Northern Rub'al-Khali, United Arab Emirates, Arabia." *Journal of the Geological Society* 176, no. 2: 269–283. https://doi.org/10.1144/jgs2017-044.

Fliocoteaux, R., M.-V. Latil-Brunt, and L. Michaud. 1988. "Histoire de la subsidence post-rift du bassin cotier mauritano-senegalo-guineen. Relation avec l'amincissement crustal pendant ia periode jurassique Cretace inferieur. Comparaison avec l'evolution des marges peri-atlantiques auniveau de l'Atlantique Central et Equatorial (cote est des U.S.A., Sud-Sahara, Cote d'Ivoire et Plateau du Demerara)." *Journal of African Earth Sciences* 7, no. 2: 345–359.

Fullgraf, T., P. M. Ndiaye, O. Blein, et al. 2013. "Silurian Magmatism in Eastern Senegal and Its Significance for the Palaeozoic Evolution of NW-Gondwana." *Journal of African Earth Sciences* 78: 66–85. https://doi.org/10.1016/j.jafrearsci.2012.08.003.

GEBCO Compilation Group. 2021. "GEBCO Grid." https://doi.org/10.5285/c6612cbe-50b3-0cff-e053-6c86abc09f8f.

Gerson, J. R., C. T. Driscoll, H. Hsu-Kim, and E. S. Bernhardt. 2018. "Senegalese Artisanal Gold Mining Leads to Elevated Total Mercury and Methylmercury Concentrations in Soils, Sediments, and Rivers." *Elementa Science of the Anthropocene* 6: 11. https://doi.org/10.1525/elementa.274.

Globig, J., M. Fernàndez, M. Torne, J. Vergés, A. Robert, and C. Faccenna. 2016. "New Insights Into the Crust and Lithospheric Mantle Structure of Africa From Elevation, Geoid, and Thermal Analysis." *Journal Geophysical Research Solid Earth* 121: 5389–5424. https://doi.org/10.1002/2016JB012972.

Gouiza, M., G. Bertotti, R. Charton, K. Haimoudane, I. Dunkl, and A. Anczkiewicz. 2019. "New Evidence of 'Anomalous' Vertical Movements Along the Hinterland of the Atlantic NW African Margin." *Journal of Geophysical Research: Solid Earth* 124, no. 12: 13333–13353. https://doi.org/10.1029/2019JB017914.

Gueye, M., S. Siegesmund, K. Wemmer, et al. 2007. "New Evidences for an Early Birimian Evolution in the West African Craton: An Example From the Kédougou-Kénieba Inlier, Southeast Senegal." *South African Journal of Geology* 110: 511–534. https://doi.org/10.2113/gssajg.110.4.511.

Haq, B. U., and B. T. Huber. 2017. "Anatomy of a Eustatic Event During the Turonian (Late Cretaceous) hot Greenhouse Climate." *Science China Earth Sciences* 60: 20–29. https://doi.org/10.1007/s11430-016-0166-y.

Hathon, E. 2018. "The SNE Discovery Offshore Senegal-Moving a Frontier Basin to Emergent." In *80th EAGE Conference and Exhibition 2018*, vol. 2018, 1–5. Utrecht, the Netherlands: European Association of Geoscientists & Engineers. https://doi.org/10.3997/2214-4609.201800712.

Hawie, N., H. Al-Wazzan, S. Al-Ali, and G. Al-Sahlan. 2021. "De-Risking Hydrocarbon Exploration in Lower Jurassic Carbonate Systems of Kuwait Through Forward Stratigraphic Models." *Marine and Petroleum Geology* 123: 104700. https://doi.org/10.1016/j.marpetgeo.2020.104700.

Hawie, N., R. Deschamps, D. Granjeon, et al. 2015. "Multi-Scale Constraints of Sediment Source to Sink Systems in Frontier Basins: A Forward Stratigraphic Modelling Case Study of the Levant Region." *Basin Research* 1-28: 418–445. https://doi.org/10.1111/bre.12156.

Hay, W. W. 2009. "Cretaceous oceans and ocean modelling. Cretaceous Oceanic Red Beds: Stratigraphy, Composition, Origins, and Paleoceanographic and Paleoclimatic Significance." SEPM Special Publication, No. 91, pp. 243–271.

Hay, W. W., R. M. DeConto, P. de Boer, S. Flogel, Y. Song, and A. Stepashko. 2019. "Possible Solutions to Several Enigmas of Cretaceous Climate." *International Journal of Earth Science* 108: 587–620. https://doi.org/10.1007/s00531-018-1670-2.

Hay, W. W., and S. Floegal. 2012. "New Thoughts About the Cretaceous Climate and Oceans." *Earth-Science Reviews* 115, no. 4: 262–272. https://doi.org/10.1016/j.earscirev.2012.09.008.

Heimhofer, U., N. Wucherpfennig, T. Adatte, et al. 2018. "Vegetation Response to Exceptional Global Warmth During Oceanic Anoxic Event 2." *Nature Communications* 9, no. 3832. https://doi.org/10.1038/s41467-018-06319-6.

Held, I. M., and B. J. Soden. 2000. "Water Vapor Feedback and Global Warming." *Annual Review of Energy and the Environment* 25: 441–475. https://doi.org/10.1146/annurev.energy.25.1.441.

Hillenbrand, I. W., and M. L. Williams. 2021. "Paleozoic Evolution of Crustal Thickness and Elevation in the Northern Appalachian Orogen, USA." *Geology* 49, no. 8: 946–951. https://doi.org/10.1130/G48705.1.

Hu, F., F. Wu, J. B. Chapman, M. N. Ducea, W. Ji, and S. Liu. 2020. "Quantitatively Tracking the Elevation of the Tibetan Plateau Since the Cretaceous: Insights From Whole-Rock Sr/Y and La/Yb Ratios." *Geophysical Research Letters* 47. https://doi.org/10.1029/2020GL089202.

Knox, R., M. Soliman, and M. Essa. 2011. "Heavy Mineral Stratigraphy of Palaeozoic and Mesozoic Sandstones of Southwestern Sinai, Egypt: A Reassessment." *GeoArabia* 16, no. 3: 31–64. https://doi.org/10.2113/geoarabia160331.

Ko, J. 2018. "Petroleum Geology of the Mauritania, Senegal, The Gambia, Guinea-Bissau, and Guinea-Conakry (MSGBC) Basin in the Northwest African Atlantic Margin." *Korean Society of Mineral and Energy Resources Engineers* 55: 478–490. https://doi.org/10.32390/ksmer.2018.55.5.478.

Krippner, A., G. Meinhold, A. C. Morton, E. Russell, and H. V. Eynatten. 2015. "Grain-Size Dependence of Garnet Composition Revealed by Provenance Signatures of Modern Stream Sediments From the Western Hohe Tauern (Austria)." *Sedimentary Geology* 321: 25–38. https://doi.org/10.1016/j.sedgeo.2015.03.002.

Latimer, J. C., G. M. Filippelli, I. L. Hendy, J. D. Gleason, and J. D. Blum. 2006. "Glacial-Interglacial Terrigenous Provenance in the Southeastern Atlantic Ocean: The Importance of Deep-Water Sources and Surface Currents." *Geology* 34, no. 7: 545–548. https://doi.org/10.1130/G22252.1.

Ledru, P., J. Pons, J. P. Milési, J. L. Feybesse, and V. Johan. 1991. "Transcurrent Tectonics and Polycyclic Evolution in the Lower Proterozoic of Senegal-Mali." *Precambrian Research* 50: 337–354.

Lewin, A., G. Meinhold, M. Hinderer, E. L. Dawit, R. Bussert, and N. K. Lünsdorf. 2020. "Heavy Minerals as Provenance Indicator in Glaciogenic Successions: An Example From the Palaeozoic of Ethiopia." *Journal of African Earth Sciences* 165: 103813. https://doi.org/10.1016/j.jafrearsci.2020.103813.

Li, Z.-H., H.-J. Qu, and W.-B. Gong. 2015. "Late Mesozoic Basin Development and Tectonic Setting of the Northern North China Craton." *Journal of Asian Earth Sciences* 114, no. 1: 115–139. https://doi.org/10.1016/j.jseaes.2015.05.029.

Long, A., and N. Cameron. 2016. "Gravity and Magnetic Constraints and Limitations in Defining Basin Structure, Offshore Senegal." Petex 2016, Poster.

Mange, M. A., and A. C. Morton. 2007. "Geochemistry of Heavy Minerals." *Developments in Sedimentology* 58: 345–391. https://doi.org/10.1016/S0070-4571(07)58013-1.

Markwitz, V., A. A. H. Kim, and J. Miller. 2015. "Compilation of West African Mineral Deposits: Spatial Distribution and Mineral Endowment." *Precambrian Research* 274: 61–81.

Martin, L., I. Effimoff, J. Medou, and M. Laughland. 2010. "Hydrocarbon Prospectivity of Offshore Senegal—Unlocking the Door to a New Deepwater Petroleum Province: AAPG Convention, New Orleans, Louisiana, April 11–14, 2010, Search and Discovery Article #10278".

Marzoli, A., S. Callegaro, J. Dal Corso, et al. 2018. "The Central Atlantic Magmatic Province (CAMP): A Review." *Late Triassic World* 46: 91–125. https://doi.org/10.1007/978-3-319-68009-5_4.

Marzoli, A., P. Renne, E. Piccirillo, M. Ernesto, G. Bellieni, and A. De Min. 1999. "Extensive 200-Million-Year-Old Continental Flood Basalts of the Central Atlantic Magmatic Province." *Science* 284, no. 5414: 616–618. https://doi.org/10.1126/science.284.5414.616.

Milési, J. P., P. Ledru, J. L. Feybesse, A. Dommanget, and E. Marcoux. 1992. "Early Proterozoic Ores Deposits and Tectonics of the Birimian Orogenic Belt, West Africa." *Precambrian Research* 58: 305–344.

Morton, A. 2012. "Value of Heavy Minerals in Sediments and Sedimentary Rocks for Provenance, Transport History and Stratigraphic Correlation." *Mineralogical Association of Canada Short Course Series* 42: 133–165.

Morton, A. C. 1985. "Heavy Minerals in Provenance Studies." *Provenance of Arenites* 148: 249–277. https://doi.org/10.1007/978-94-017-2809-6_12.

Morton, A. C. 1986. "Dissolution of Apatite in North Sea Jurassic Sandstones: Implications for the Generation of Secondary Porosity." *Clay Minerals* 21, no. 4: 711–733. https://doi.org/10.1180/claymin.1986.021.4.16.

Morton, A. C., J. I. Chisholm, and D. Frei. 2024. "Provenance Response to Evolving Palaeogeography Recorded by Carboniferous Sandstones in the Northern Pennine Basin, UK." *Sedimentary Geology* 470: 106691. https://doi.org/10.1016/j.sedgeo.2024.106691.

Morton, A. C., and C. Hallsworth. 1994. "Identifying Provenance-Specific Features of Detrital Heavy Mineral Assemblages in Sandstones." *Sedimentary Geology* 90, no. 3–4: 241–256. https://doi.org/10.1016/0037-0738(94)90041-8.

Morton, A. C., and C. R. Hallsworth. 1999. "Processes Controlling the Composition of Heavy Mineral Assemblages in Sandstones." *Sedimentary Geology* 124: 3–29. https://doi.org/10.1016/s0037-0738(98)00118-3.

Morton, A. C., and P. McGill. 2018. "Correlation of Hydrocarbon Reservoir Sandstones Using Heavy Mineral Provenance Signatures: Examples From the North Sea and Adjacent Areas." *Minerals* 2018, no. 8: 564. https://doi.org/10.3390/min8120564.

Mounteney, I. 2011. *The Use of Lithium Heteropolytungstate as an Alternative to Bromoform for Heavy Media Separations*. Nottingham: British Geological Survey. (IR/11/049-unpublished). https://nora.nerc.ac.uk/id/eprint/519459/.

Mounteney, I., M. Casson, J. Rushton, I. Millar, N. Dethie, and J. Redfern. 2021. "Cenozoic to Modern-Day Source to Sink Systems of Senegal: A Record of Provenance, Transport, Recycling and Climate Controls." *Journal of African Earth Sciences* 178: 104150. https://doi.org/10.1016/j.jafrearsci.2021.104150.

Mourlot, Y., G. Calves, P. D. Clift, G. Baby, A. C. Chaboureau, and F. Raisson. 2018. "Seismic Stratigraphy of Cretaceous Eastern Central Atlantic Ocean: Basin Evolution and Palaeoceanographic Implications." *Earth and Planetary Sciences Letters* 499, no. 10: 107–121. https://doi.org/10.1016/j.epsl.2018.07.023.

Mourlot, Y., M. Roddaz, G. Dera, et al. 2018. "Geochemical Evidence for Large-Scale Drainage Reorganization in Northwest Africa During the Cretaceous." *Geochemistry, Geophysics, Geosystems* 19: 1690–1712. https://doi.org/10.1029/2018GC007448.

Mulch, A., C. Teyssier, M. Cosca, O. Vanderhaeghe, and T. Vennemann. 2004. "Reconstructing Paleoelevation in Eroded Orogens." *Geology* 32: 525. https://doi.org/10.1130/G20394.1.

Nauton-Fourteu, M., S. Tyrrell, and A. Morton. 2020. "Heavy Mineral Variations in Mid-Carboniferous Deltaic Sandstones: Records of a Pre-Depositional Sediment History?" *Depositional Record* 7, no. 1: 52–63. https://doi.org/10.1002/dep2.128.

Ndiaye, M., P. M. Ngom, G. Gorin, M. Villeneuve, M. Sartori, and J. Medou. 2016. "A New Interpretation of the Deep-Part of Senegal-Mauritanian Basin in the Diourbel-Thies Area by Integrating Seismic, Magnetic, Gravimetric and Borehole Data: Implication for Petroleum Exploration." *African Earth Sciences* 121: 330–341. https://doi.org/10.1016/j.jafrearsci.2016.06.002.

Page, A. 1988. "Rock Deformation Associated With the Displacement of Allochthonous Units in the Central Segment of the Caledono-Hercynian Mauritanide Belt (Islamic Republic of Mauritania and Eastern Senegal)." *Journal of African Earth Sciences* 7, no. 1: 265–283.

Paton, C., J. Hellstrom, B. Paul, J. Woodhead, and J. Hergy. 2011. "Iolite: Freeware for the Visualisation and Processing of Mass Spectrometric Data." *Journal of Analytical Spectrometry* 26: 2508–2518. https://doi.org/10.1039/C1JA10172B.

Pearson, M., M. Casson, I. Millar, R. Charton, and J. Redfern. 2023. "Cretaceous Climate Change Evidenced in the Senegalese Rock Record, NW Africa." *Journal of African Earth Sciences* 211: 105166. https://doi.org/10.1016/j.jafrearsci.2023.105166.

Perez-Díaz, L., and G. Eagles. 2017. "South Atlantic Paleobathymetry Since Early Cretaceous." *Scientific Reports* 7: 11819. https://doi.org/10.1038/s41598-017-11959-7.

Pierrehumbert, R. T. 2002. "The Hydrologic Cycle in Deep-Time Climate Problems." *Nature* 419: 191–198. https://doi.org/10.1038/nature01088.

Pletsch, T., J. Erbacher, A. E. L. Holburn, et al. 2001. "Cretaceous Separation of Africa and South America: The View From the West African Margin (ODP Leg 159)." *Journal of South American Earth Sciences* 14: 147–174. https://doi.org/10.1016/S0895-9811(01)00020-7.

Ponsard, J. F., J. Roussel, and M. Villeneuve. 1988. "The Pan-African Orogenic Belt of Southern Mauritanides and Northern Rokelides (Southern Senegal and Guinea, West Africa): Gravity Evidence for a Collisional Suture." *Journal of African Earth Sciences* 7, no. 2: 463–472.

Poulsen, C. J., A. S. Gendaszek, and R. L. Jacob. 2013. "Did the Rifting of the Atlantic Ocean Cause the Cretaceous Thermal Maximum?" *Geology* 31, no. 2: 115–118. https://doi.org/10.1130/0091-7613(2003)031<0115:DTROTA>2.0.CO;2.

Rinaldi, M., A. M. Gurnell, M. G. del Tánago, M. Bussettini, and D. Hendriks. 2016. "Classification of River Morphology and Hydrology to Support Management and Restoration." *Aquatic Sciences* 78: 17–33. https://doi.org/10.1007/s00027-015-0438-z.

Ritz, M., and Y. Bellion. 1988. "Geologic Sections Across the Onshore Senegal -Mauritania Basin Derived From Geoelectric Studies." *Journal of Earth Sciences* 26: 65–73.

Roden-Tice, M. K., D. Eusden-Jr, and R. P. Wintsch. 2012. "Apatite Fission-Track Evidence for the Cretaceous Development of Kilometre-Scale Relief and Steady-State Tertiary Topography in New England." *Geomorphology* 141-142: 114–120. https://doi.org/10.1016/j.geomorph.2011.12.029.

Roquette, E., S. Schröder, T. Luber, S. Tyrrell, and J. Redfern. 2019. "New Constraints on Source to Sink Systems of NW Africa: Provenance Analysis of the Mesozoic Post-Rift Clastics in the Essaouira-Agadir Basin (Morocco)." Geophysical Research Abstracts 21. https://ui.adsabs.harvard.edu/abs/2019EGUGA..2110682R.

Sadio, M., E. J. Anthony, A. T. Diaw, et al. 2017. "Shoreline Changes on the Wave-Influenced Senegal River Delta, West Africa: The Roles of Natural Processes and Human Interventions." *Water* 9, no. 5: 357. https://doi.org/10.3390/w9050357.

Salard-Cheboldaeff, M., and J. Dejax. 1991. "Evidence of Cretaceous to Recent West African Intertropical Vegetation From Continental Sediment Spore-Pollen Analysis." *Journal of African Earth Sciences* 12: 353–361. https://doi.org/10.1016/0899-5362(91)90084-C.

Scherer, C. M. S., R. G. Mello, J. P. F. Ferronatto, et al. 2020. "Changes in Prevailing Surface-Palaeowinds of Western Gondwana During Early Cretaceous." *Cretaceous Research* 116: 104598. https://doi.org/10.1016/j.cretres.2020.104598.

Schlanger, S. O., and H. C. Jenkyns. 1976. "Cretaceous Oceanic Anoxic Events: Causes and Consequences." *Geologie en Mijnbouw* 55, no. 3: 179–184.

Scotese, C. R. 2016. "PALEOMAP PaleoAtlas for GPlates and the PaleoData Plotter Program, PALEOMAP Project." http://www.earthbyte.org/paleomap-paleoatlas-for-gplates/.

Suttner, L. J., and P. K. Dutta. 1986. "Alluvial Sandstone Composition and Paleoclimate 1. Framework Mineralogy." *Journal of Sedimentary Petrology* 56: 326–345.

Takashima, R., H. Nishi, B. T. Huber, and M. Leckie. 2006. "Greenhouse World and the Mesozoic Ocean." *Oceanography* 19, no. 4: 64–74. https://doi.org/10.5670/oceanog.2006.07.

Trenous, P.-Y., and P. Michel. 1971. "Etude de la structure du dome de Guier (Senegal nord-occidental)." *Bulletin de la Societe Geologique de France* 1-2: 133–139.

Vermeesch, P. 2018. "IsoplotR: A Free and Open Toolbox for Geochronology." *Geoscience Frontiers* 9: 1479–1493. https://doi.org/10.1016/j.gsf.2018.04.001.

Villeneuve, M. 2008. "Review of the Orogenic Belts on the Western Side of the West African Craton: The Bassarides, Rokelides and Mauritanides. The Boundaries of the West African Craton." *Geological Society, London, Special Publications* 297: 169–201.

Villeneuve, M., and J.-J. Cornee. 1994. "Structure, Evolution and Palaeogeography of the West African Craton and Bordering Belts During the Neoproterozoic." *Precambrian Research* 69: 307–326. https://doi.org/10.1016/0301-9268(94)90094-9.

Villeneuve, M., F. Fournier, S. Cirilli, et al. 2015. "Structure of the Paleozoic Basement in the Senegalo-Mauritanian Basin (West Africa)." *Bulletin de la Societe Geologique de France* 186: 2–3.

Villeneuve, M., H. Theveniaut, P. M. Ndiaye, and S. Retiere. 2014. "Re-Assessment of the Northern Guinean "Koubia–Lessere Unconformity" (KLU): Consequences on the Geological Correlations Throughout West Africa." *Academie Des Sciences* 346, no. 9–10: 262–272. https://doi.org/10.1016/j.crte.2014.05.004.

Weltje, G. J. 1994. "Provenance and Dispersal of Sand-Sized Sediments: Reconstruction of Dispersal Patterns and Sources of Sand-Sized Sediments Using Inverse Modelling Techniques." PhD Dissertation, Utrecht University Geologica, Prague 8, 9–32.

Supporting Information

Additional supporting information can be found online in the Supporting Information section.